Neutron diffraction instrumentation

Magnus H. Sørby

IFE

Rough division

- Neutron diffraction instruments
  - Single crystal diffractometers
    - Constant wavelenght
    - Time-of-flight (TOF)
  - Powder diffractometers
    - Constant wavelenght
    - Time-of-flight (TOF)

Single crystal diffraction

Four-circle diffractometer

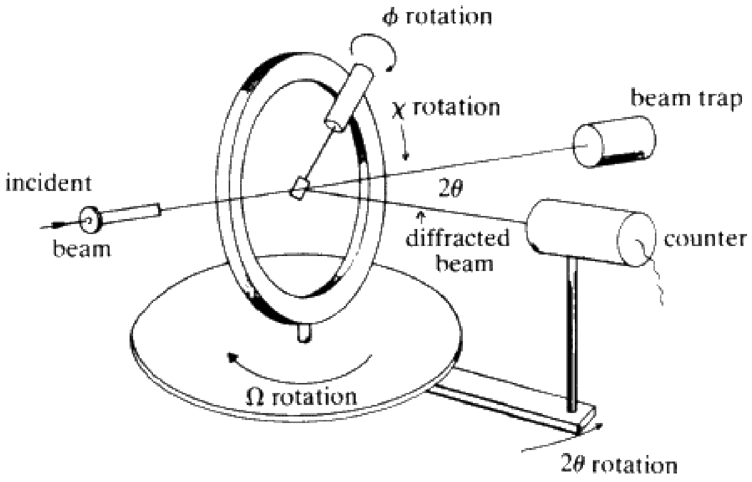

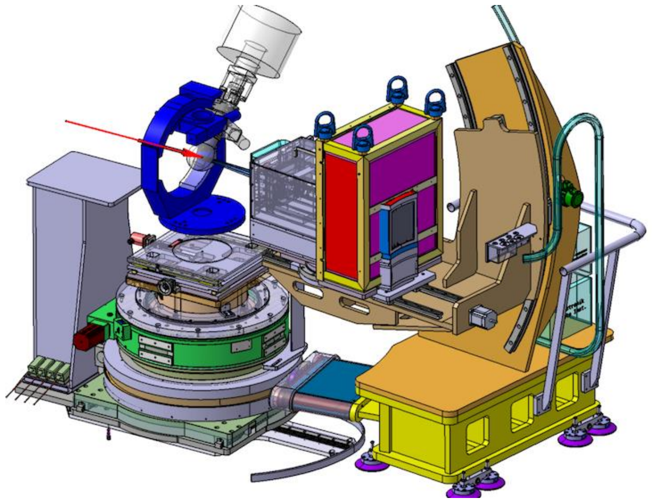

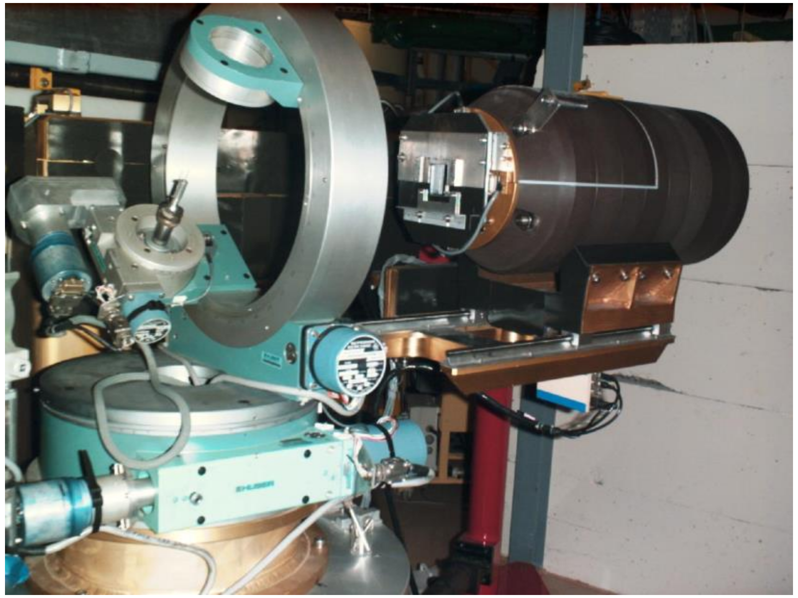

- 3-D rotation of single crystal
- Access to all reflections

- Traditionally single detector
- Now: also 1D and 2D detectors

Neutrons from nuclear reactors – constant wavelength experiments

$$\lambda = 2d\sin\theta$$

$fixed$

JEEP II reactor, IFE spectrum

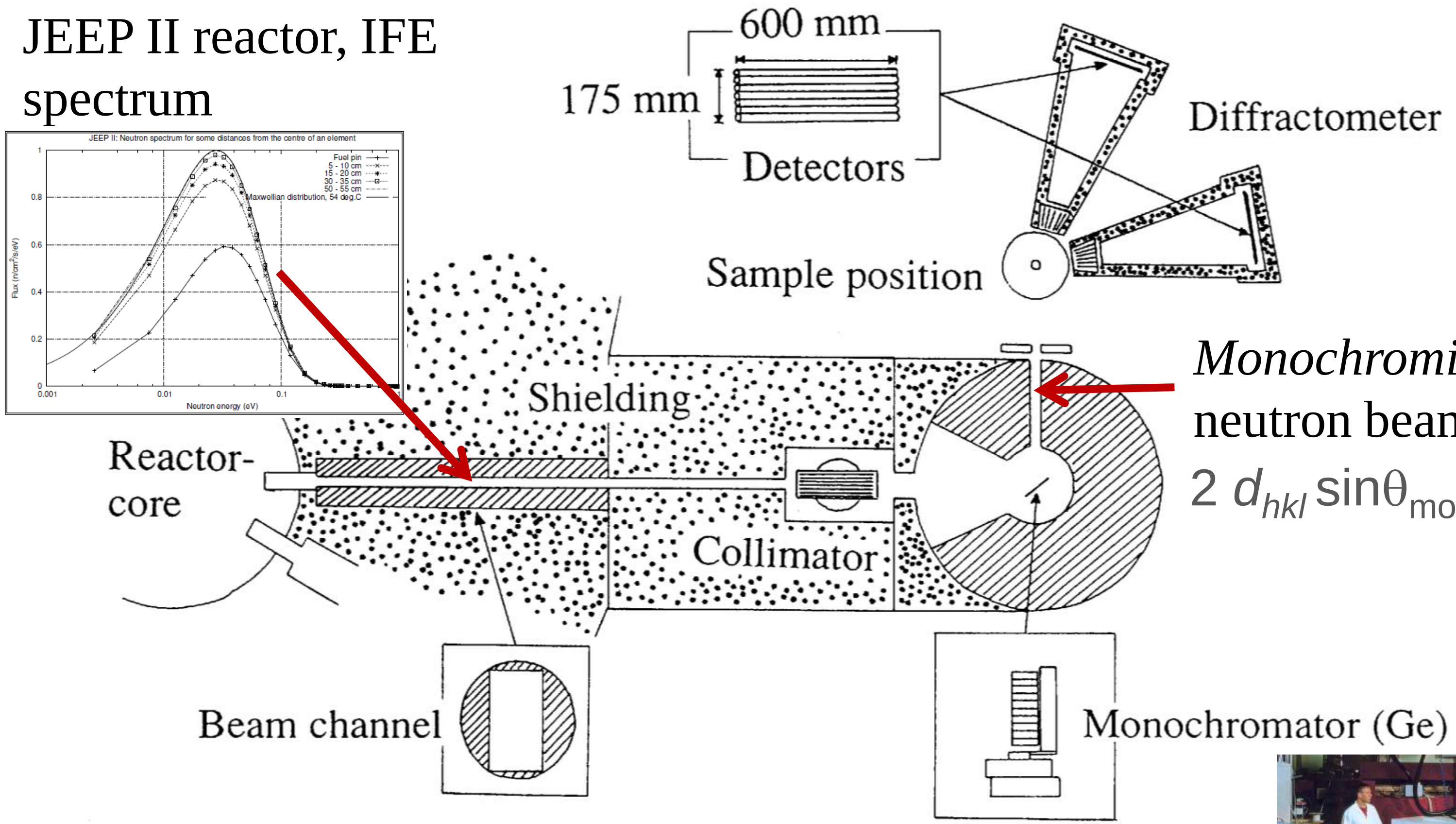

Monochromic
neutron beam

$2\, d_{hkl} \sin\theta_{monochr} = \lambda$

PUS – a high resolution diffractometer

- In operation 1997-2019

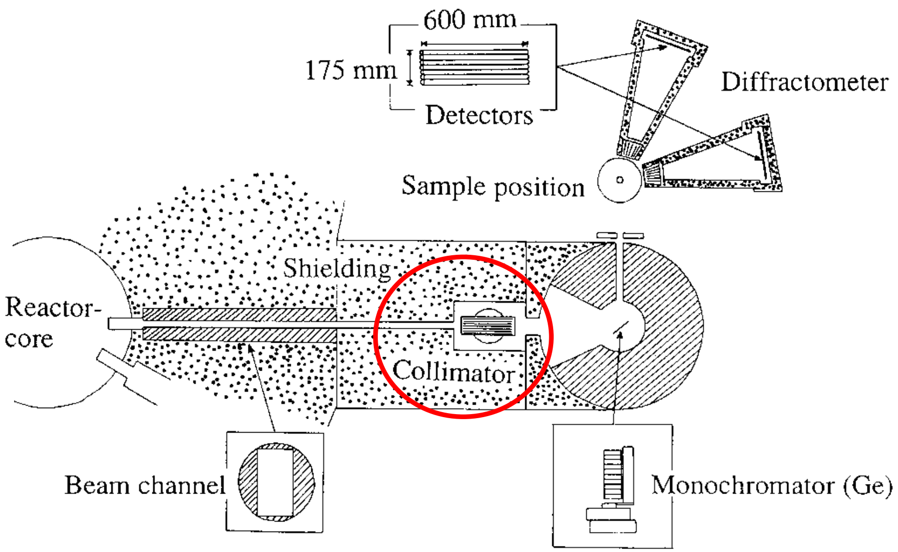

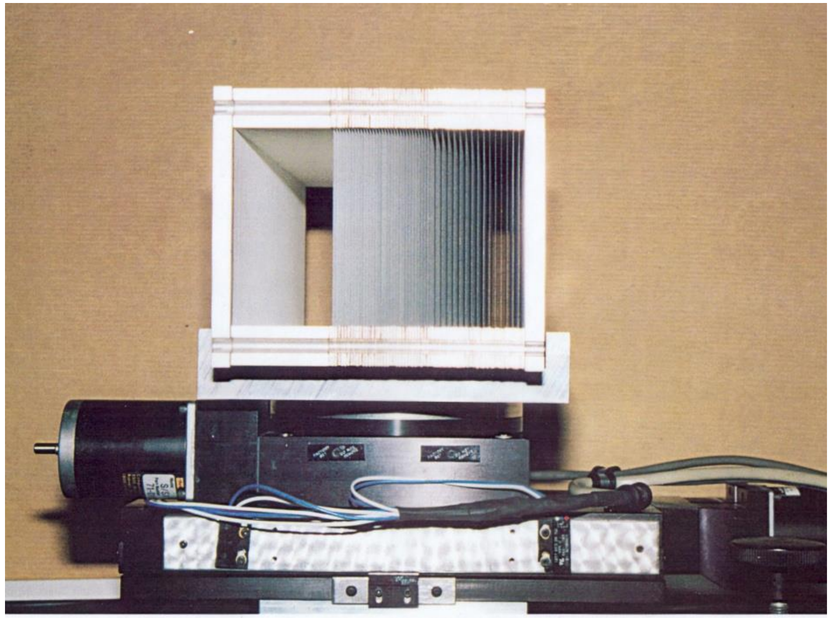

Soller collimator (from Risø).
15’, 30’ and “open” (60’)

PUS – a high resolution diffractometer

- In operation 1997-2019

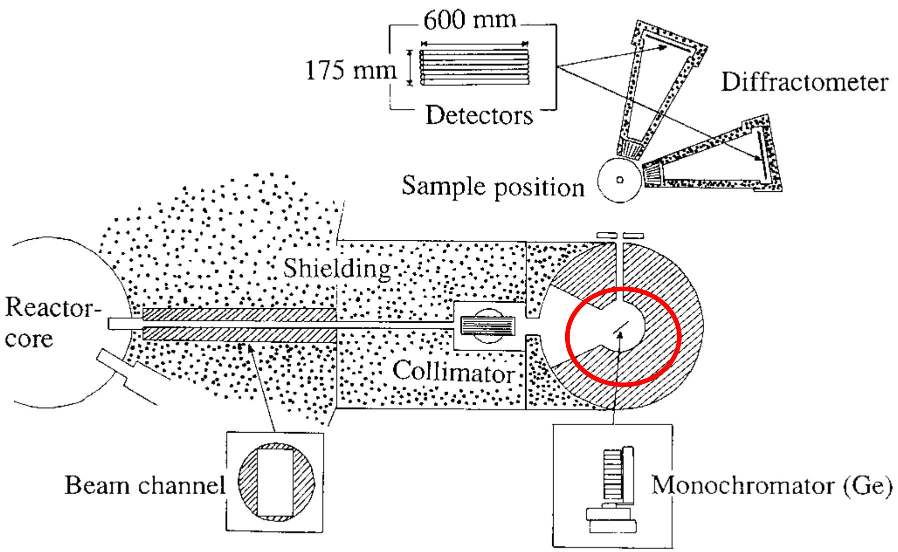

Vertically focusing Ge monochromator (from Risø).

311, 511 or 711 reflection plane can be used → λ = 0.75-2.60 Å

Mosaic crystal – ideally imperfect crystal

Model of real crystal:

- Mosaic of crystalline blocks
- Each dimensions μm tilted very slightly to each other

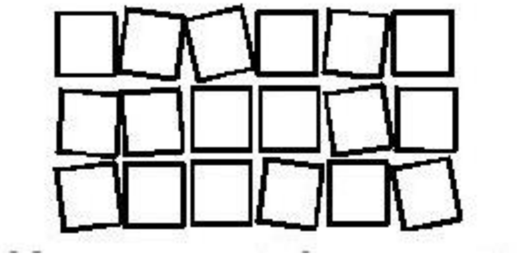

Mosaic model of crystal

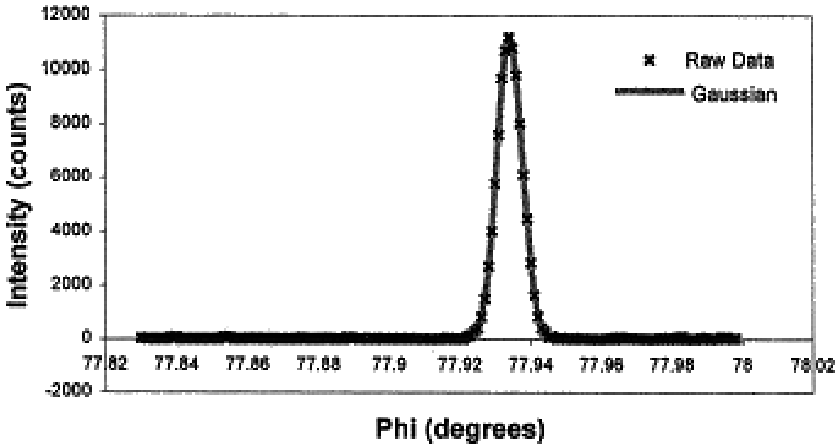

Perfect crystal

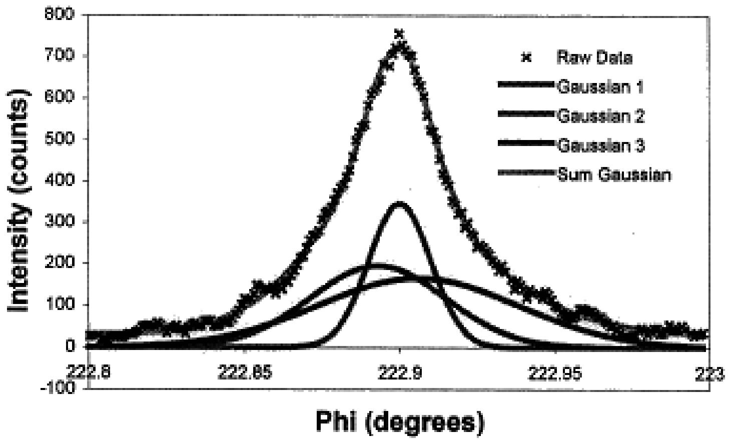

Mosaic crystal

PUS – a high resolution diffractometer

- In operation 1997-2019

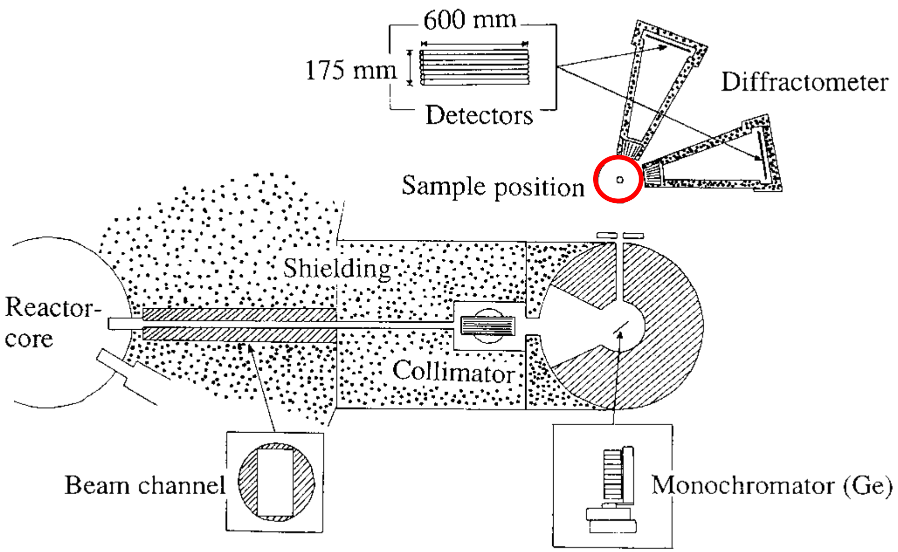

Sample temperature: 8 – 1200K

Gas pressures up to 8 bar

PUS – a high resolution diffractometer

- In operation 1997-2019

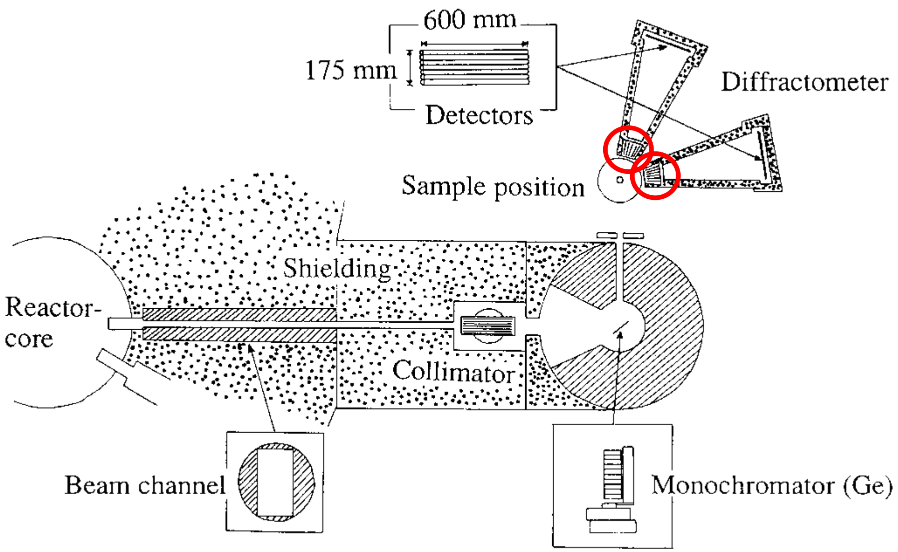

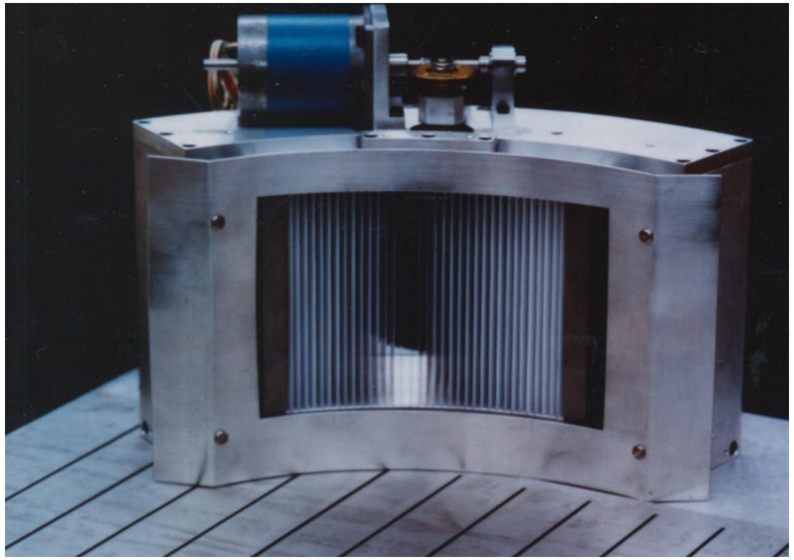

Oscillating radial collimators (MURR).

PUS – a high resolution diffractometer

- In operation 1997-2019

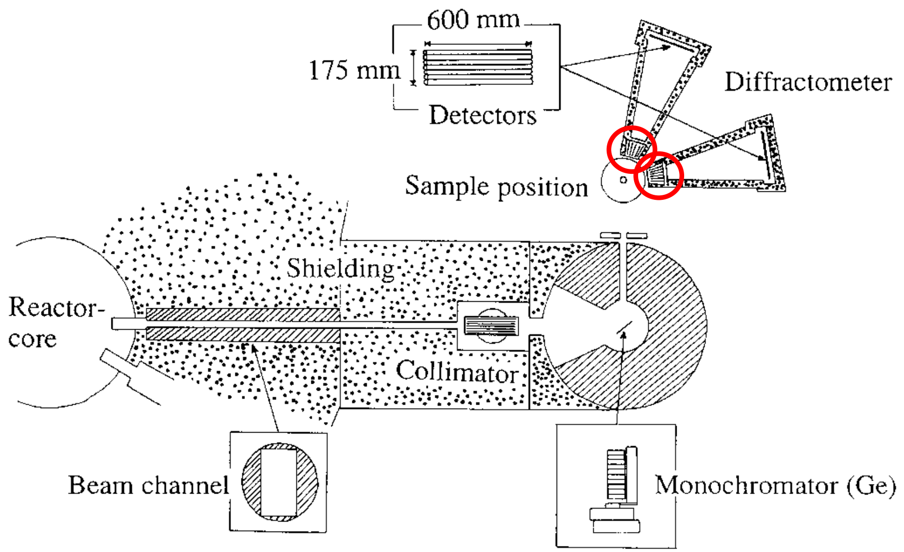

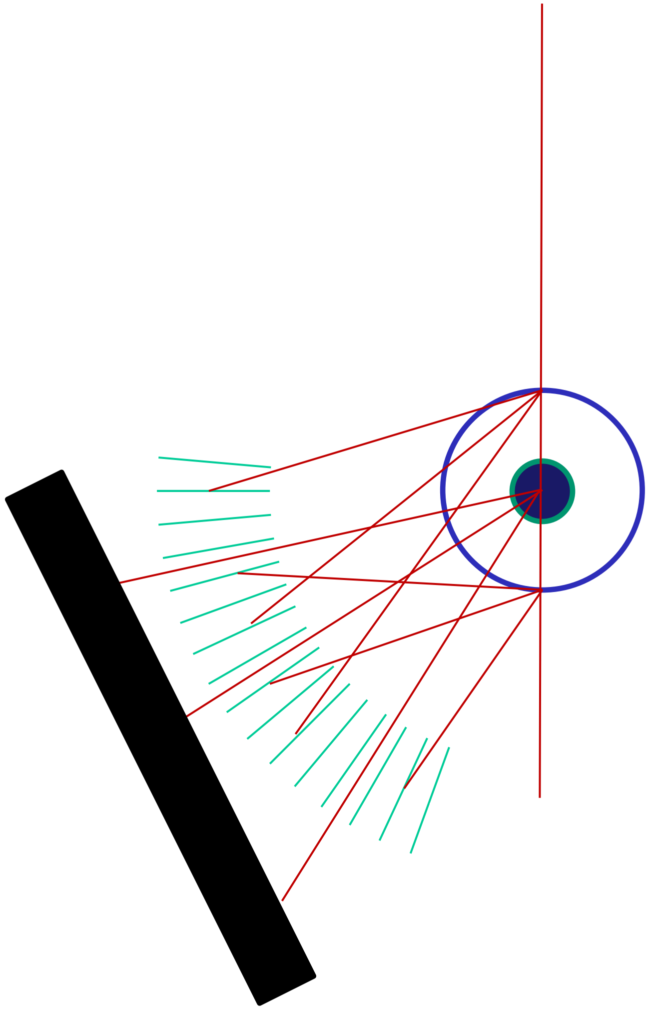

PUS – a high resolution diffractometer

- In operation 1997-2019

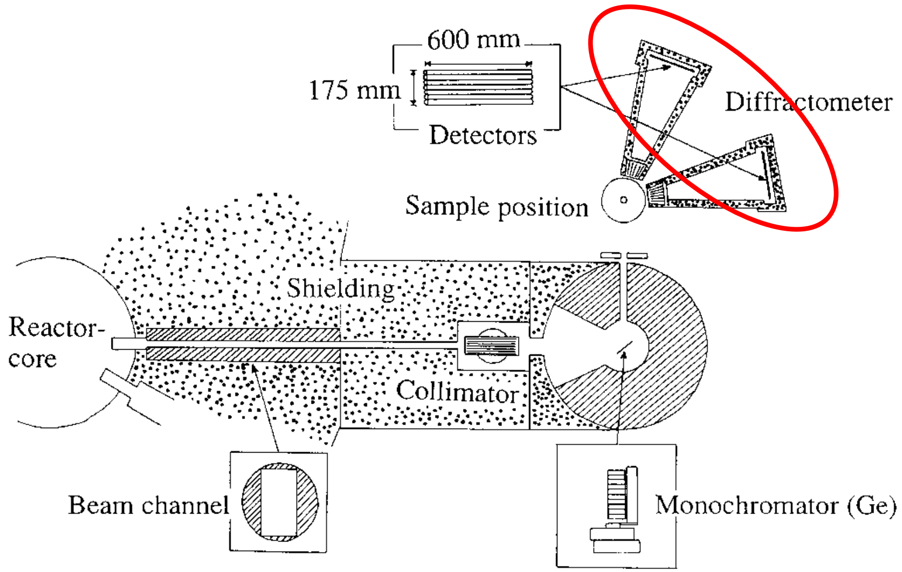

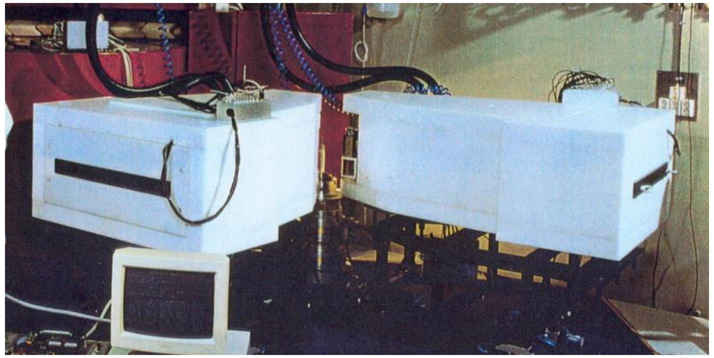

2 detector banks with 7 vertically stacked position sensitive detectors in each. Each bank cover 20º scattering angle.

Time-of-flight diffraction (spallation)

$$\lambda = 2d \sin\theta$$

θ: $fixed$

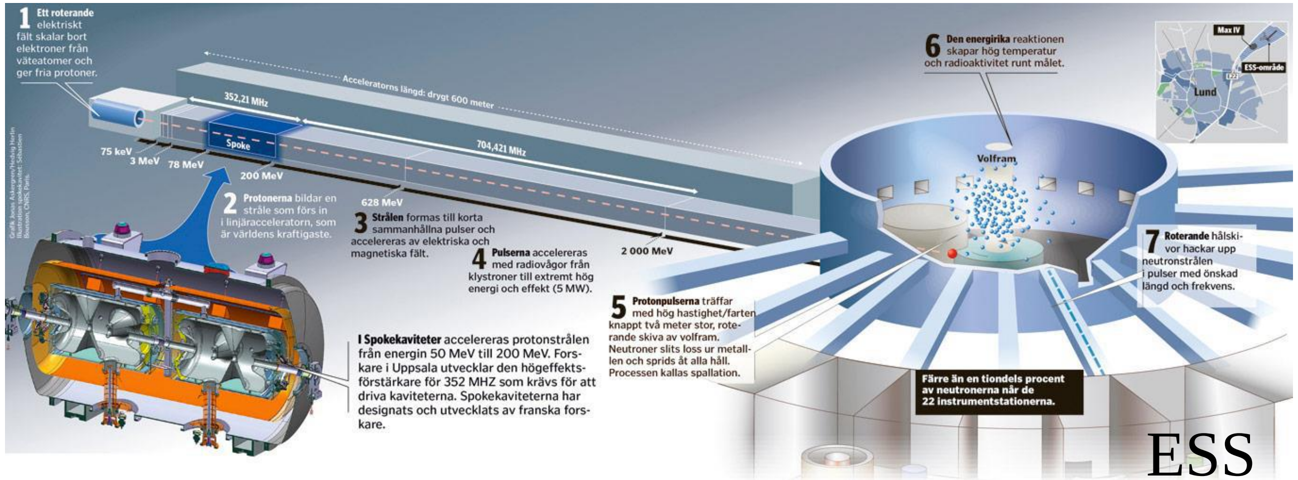

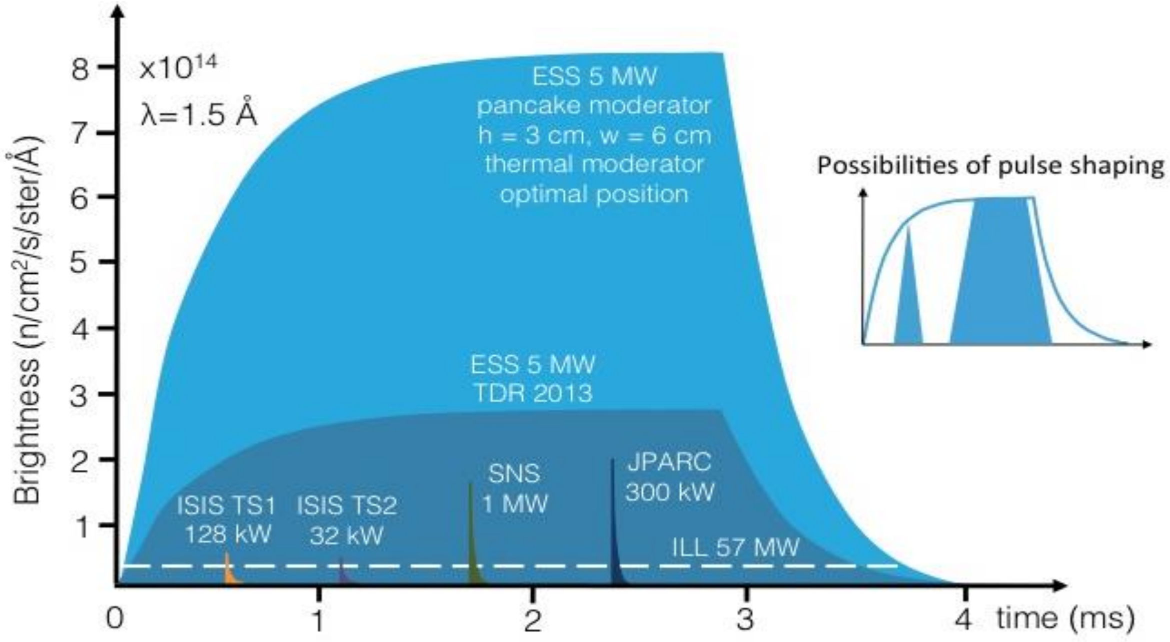

Time-of-flight diffraction (spallation)

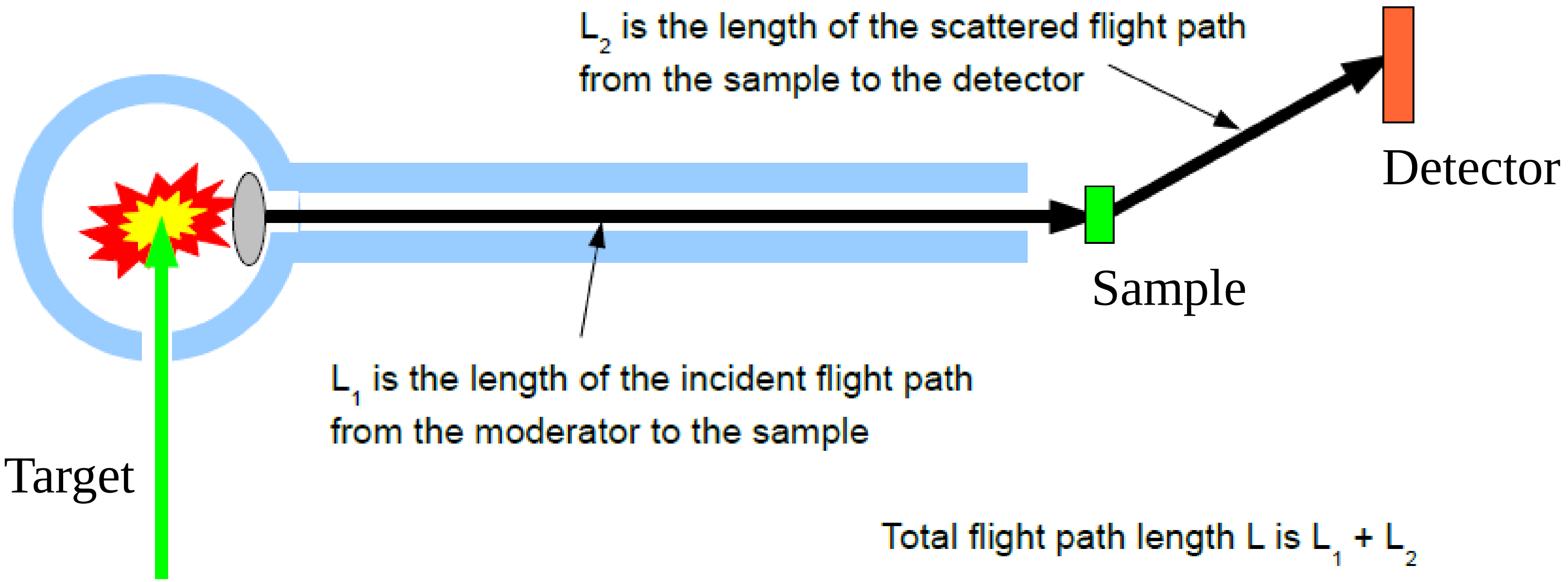

Sample irradiated by a pulsed neutron beam with wide range of wavelengths.
Because pulsed beam $\Rightarrow$ different wavelengths can be sorted by their time of arrival at the detector.

Time-of-flight diffraction (spallation)

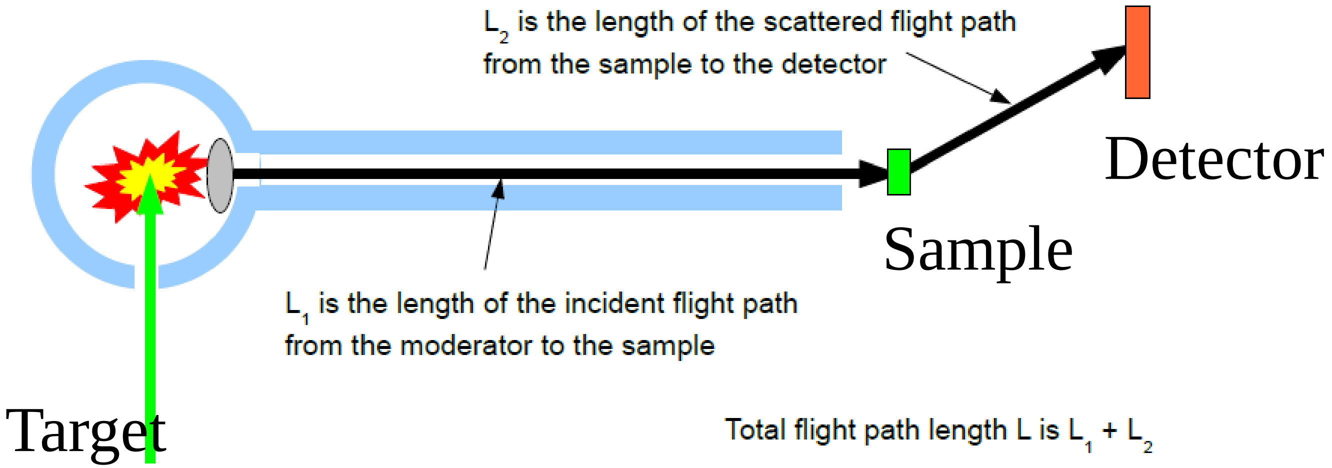

de Broglie expression:

$$\frac{h}{\lambda} = m_n v = m_n\left(\frac{L}{t}\right)$$

t (μsec) = 252.78 L (m) λ (Å)

h: Planck' constant
λ: wavelength
m_n: mass neutron
v: velocity
t: time (L path length)

$$\boxed{\lambda = \frac{ht}{m_n L}} + \boxed{\lambda = 2d\sin\theta} \Rightarrow \boxed{d = \frac{h}{2m_n L \sin\theta}\, t}$$

Time-of-flight diffraction (spallation)

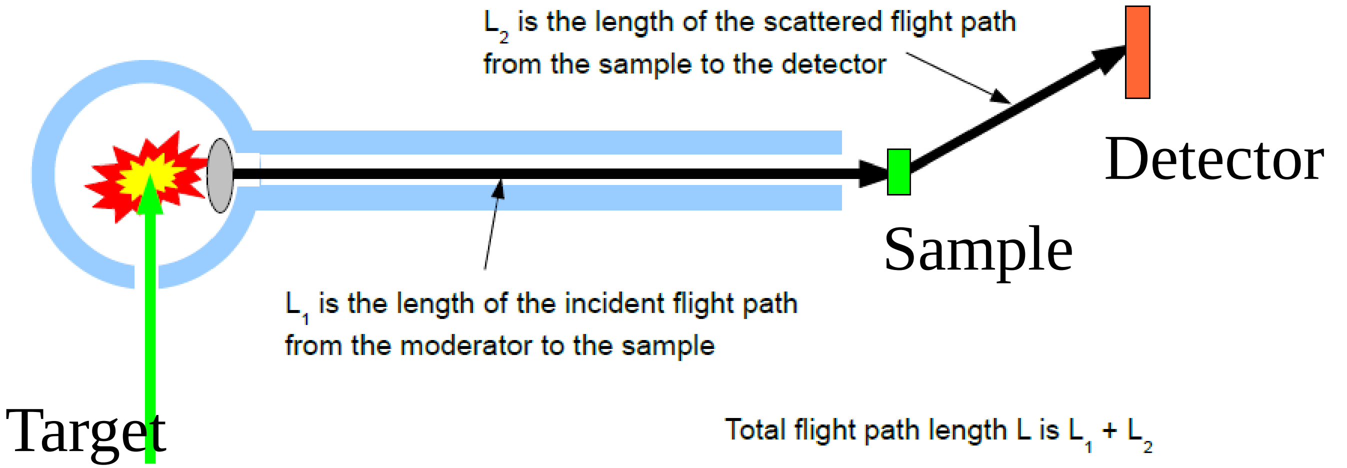

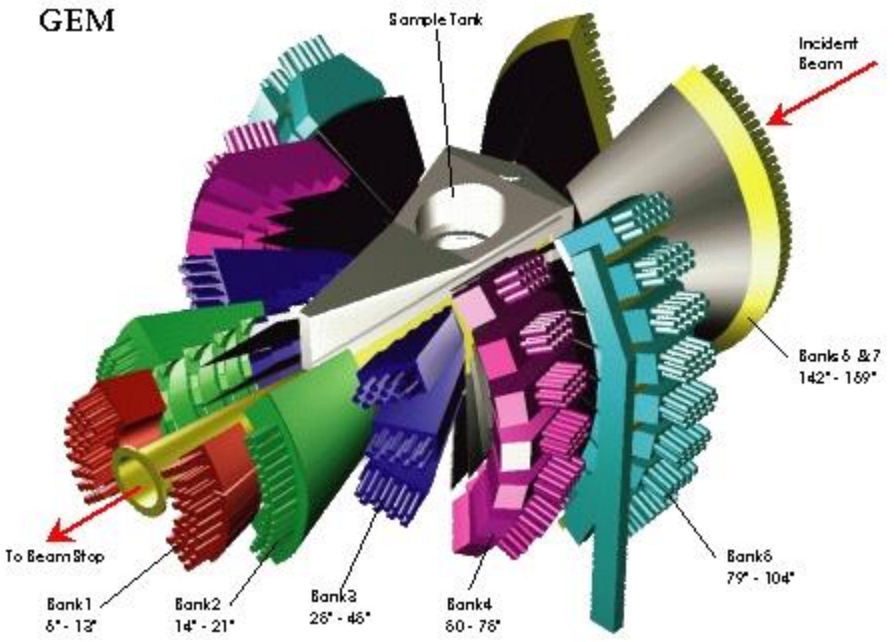

POLARIS at ISIS

Time-of-flight diffraction (spallation)

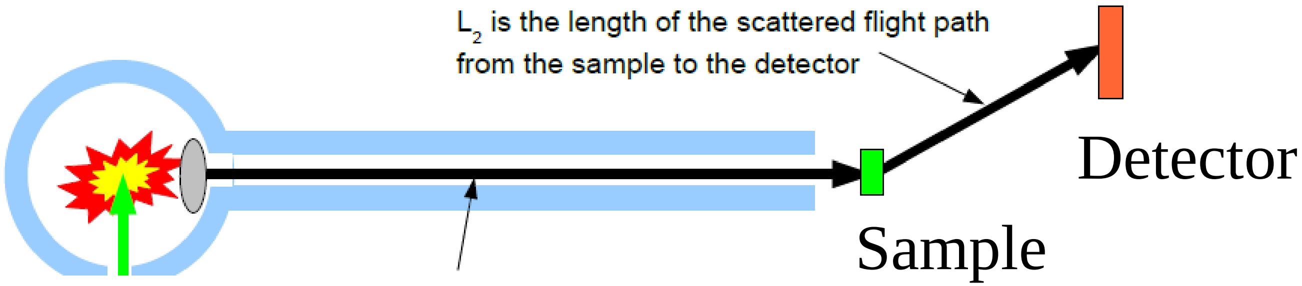

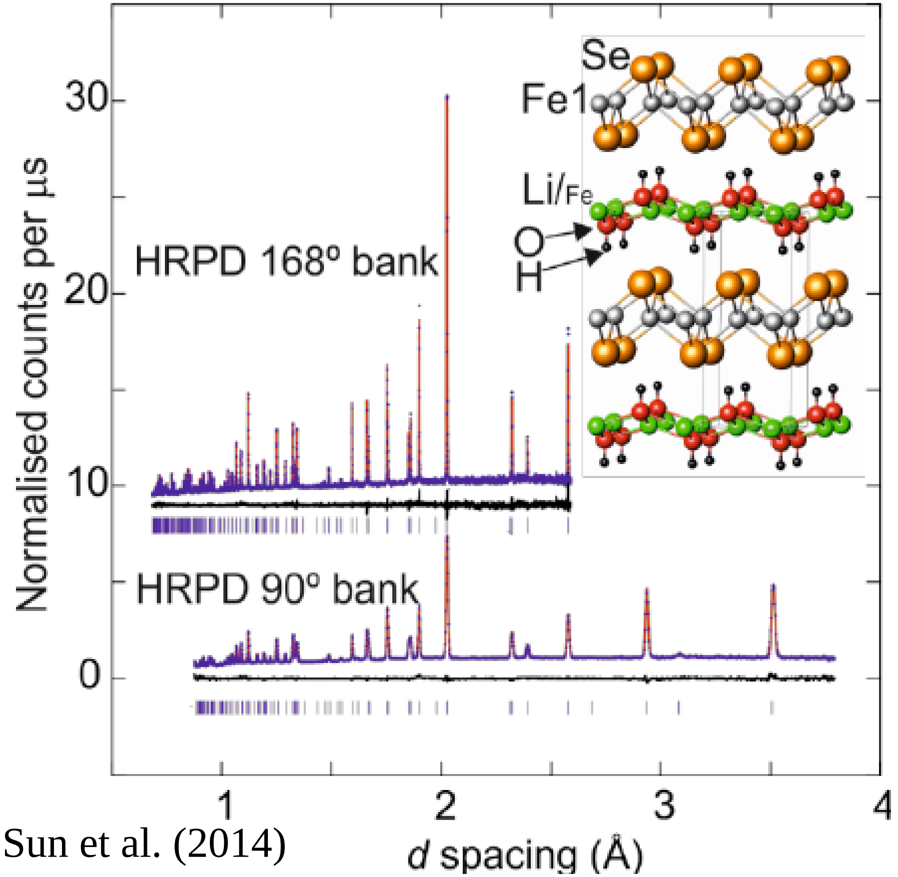

Sun et al. (2014)

<u>HRPD at ISIS</u>

- $L_1 = 96$ m

$$\Delta d/d = \sqrt{\left(\frac{\Delta\theta}{\tan(\theta)}\right)^2 + \left(\frac{\Delta t}{t}\right)^2 + \left(\frac{\Delta L}{L}\right)^2}$$

$$= 4 * 10^{-4}$$

Time-of-flight diffraction (reactor)

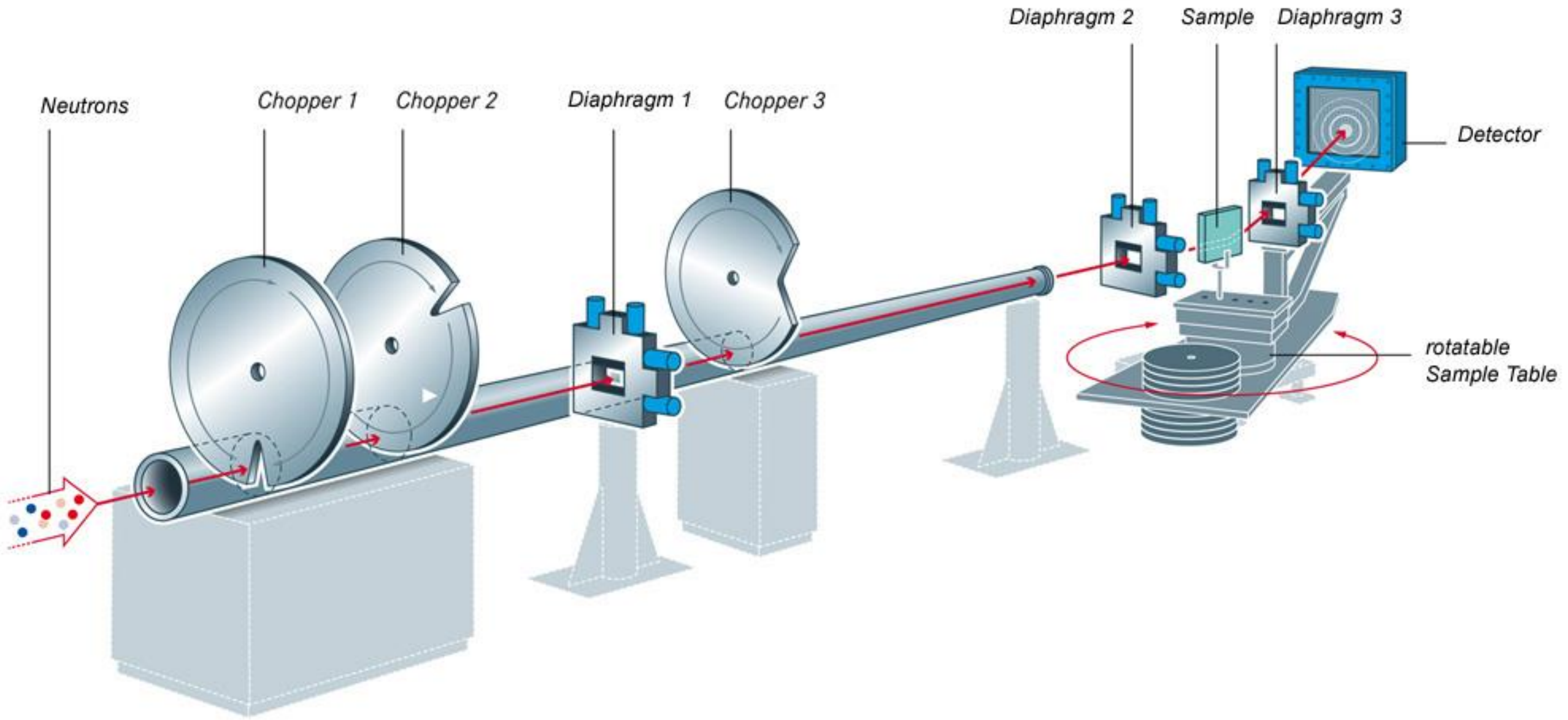

Use of chopper(s)

Total scattering

Outline

- Bragg scattering and “the average picture”
- Total scattering and Reverse Monte Carlo (RMC) modeling
- RMC modeling of interstitial deuterides

Analysis of powder diffraction data

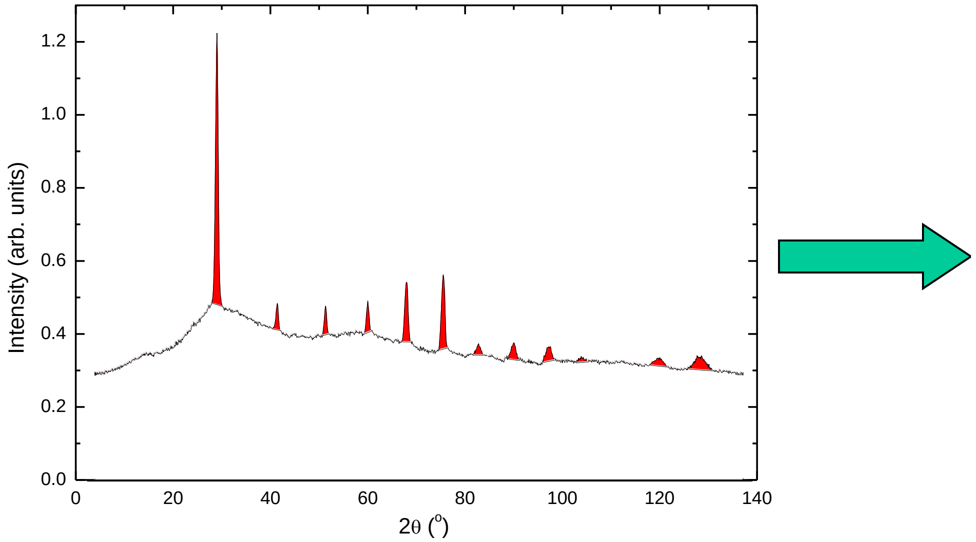

Bragg scattering

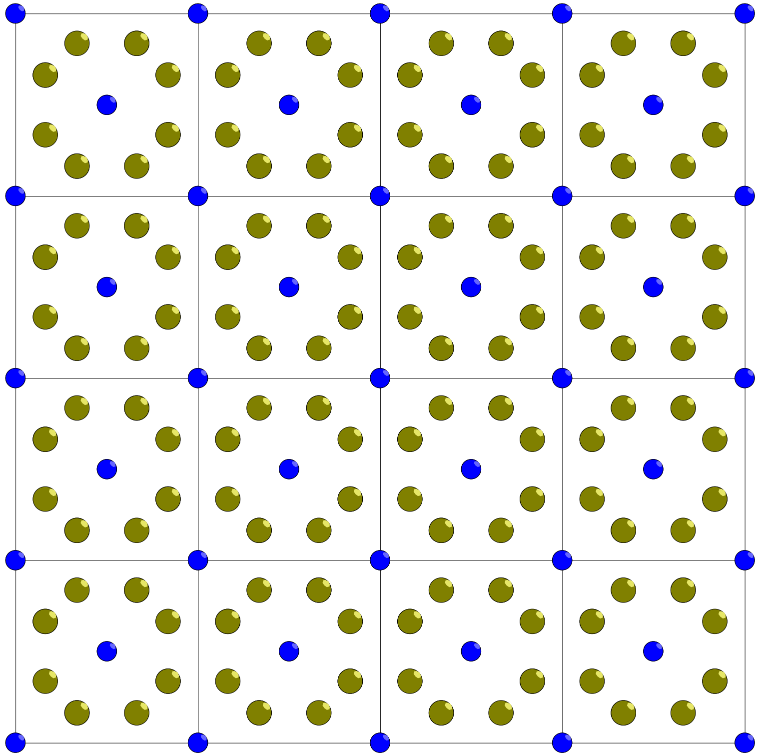

- a perfectly periodic model

Analysis of powder diffraction data

Materials are not perfectly periodic!

- thermal motion
- defects
- non-stoichiometry
- occupational disorder

.

.

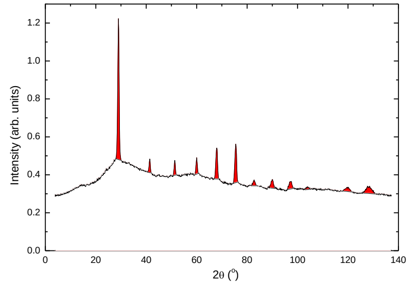

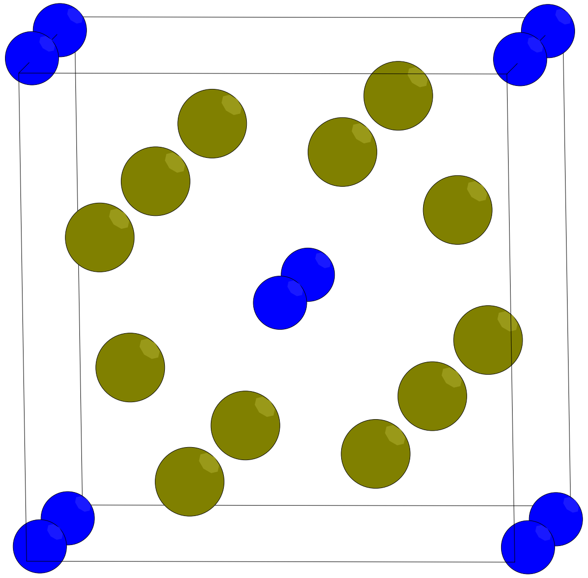

Analysis of powder diffraction data

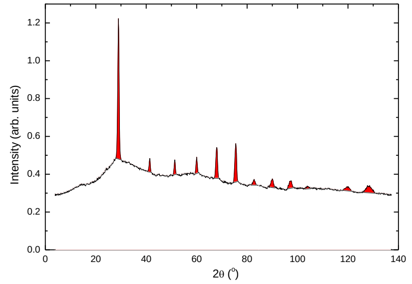

Materials are not perfectly periodic!

- thermal motion
- defects
- non-stoichiometry
- occupational disorder

.

.

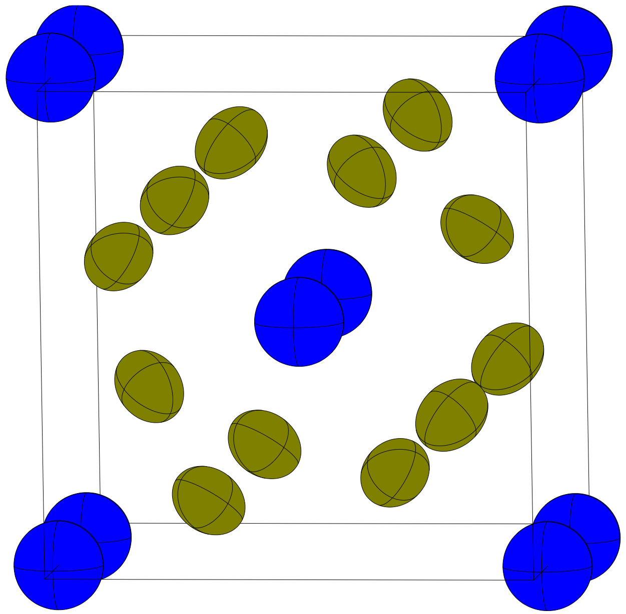

Analysis of powder diffraction data

Materials are not perfectly periodic!

- thermal motion
- defects
- non-stoichiometry
- occupational disorder

.

.

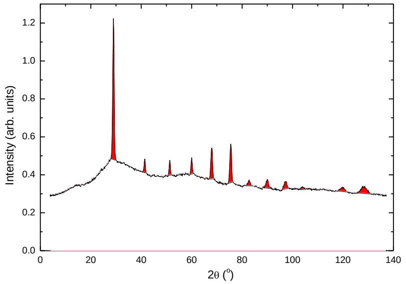

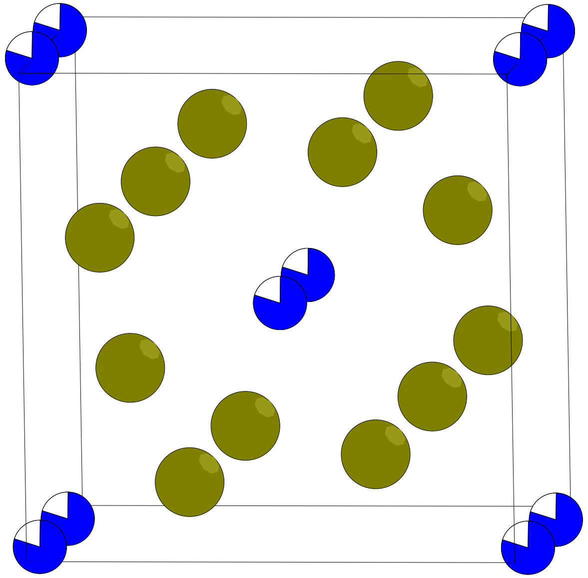

Is the average picture good enough???

It depends ......

- on the material we are interested in.
- on what we want to know about it.

- A parallell from the macrosocpic world:
  - a study of audiences

A well-ordered audience

Questions we can answer from the average picture:

- What is the typical distance between two persons?
- What do they wear?

A more disordered audience

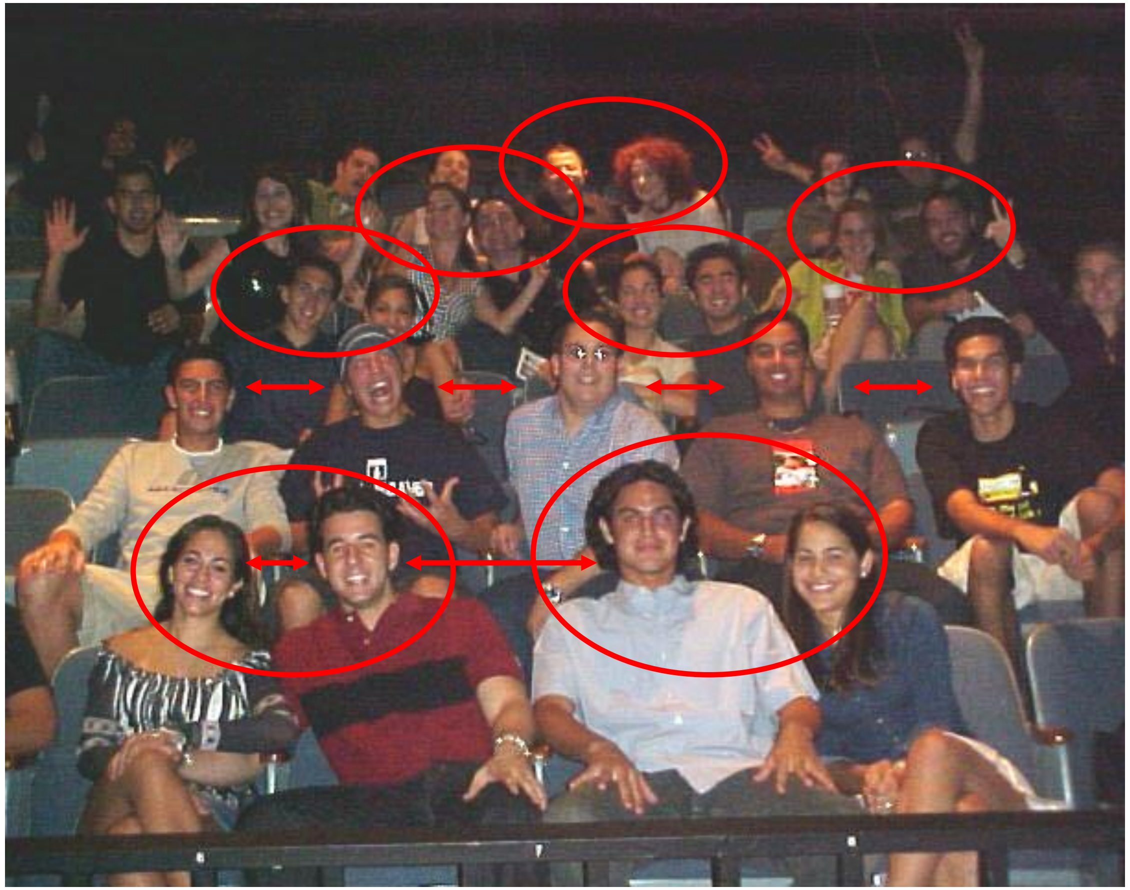

Questions we cannot answer from the average picture:

- What is the typical distance between two persons?
- What do they wear?

The average picture of a metal hydride

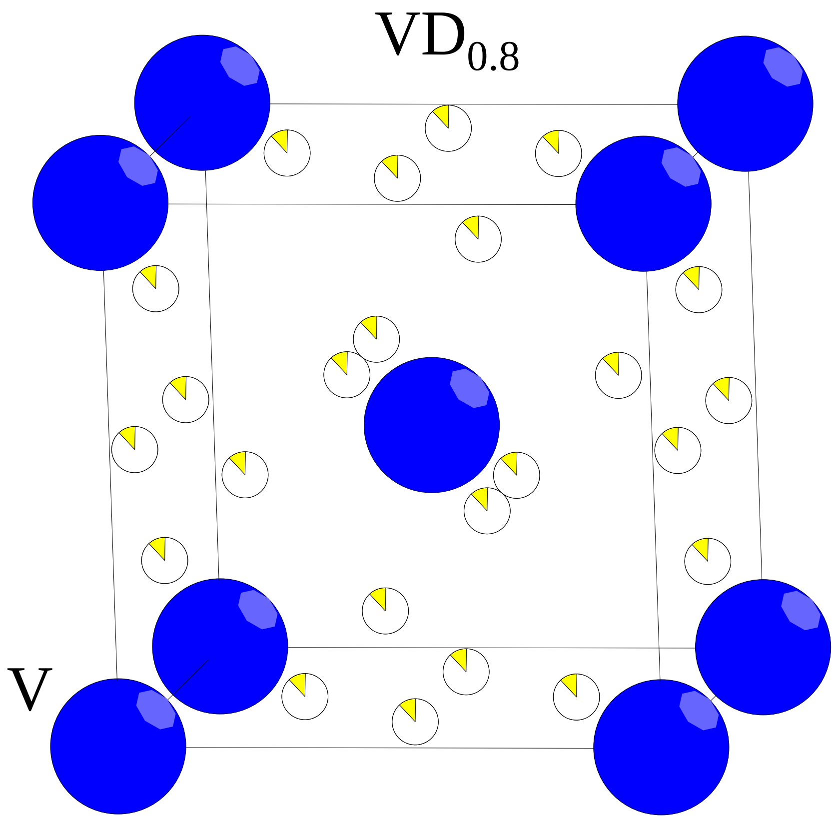

Question we can answer:

- How do the hydrogen atoms relate to the metal atoms?

The average picture of a metal hydride

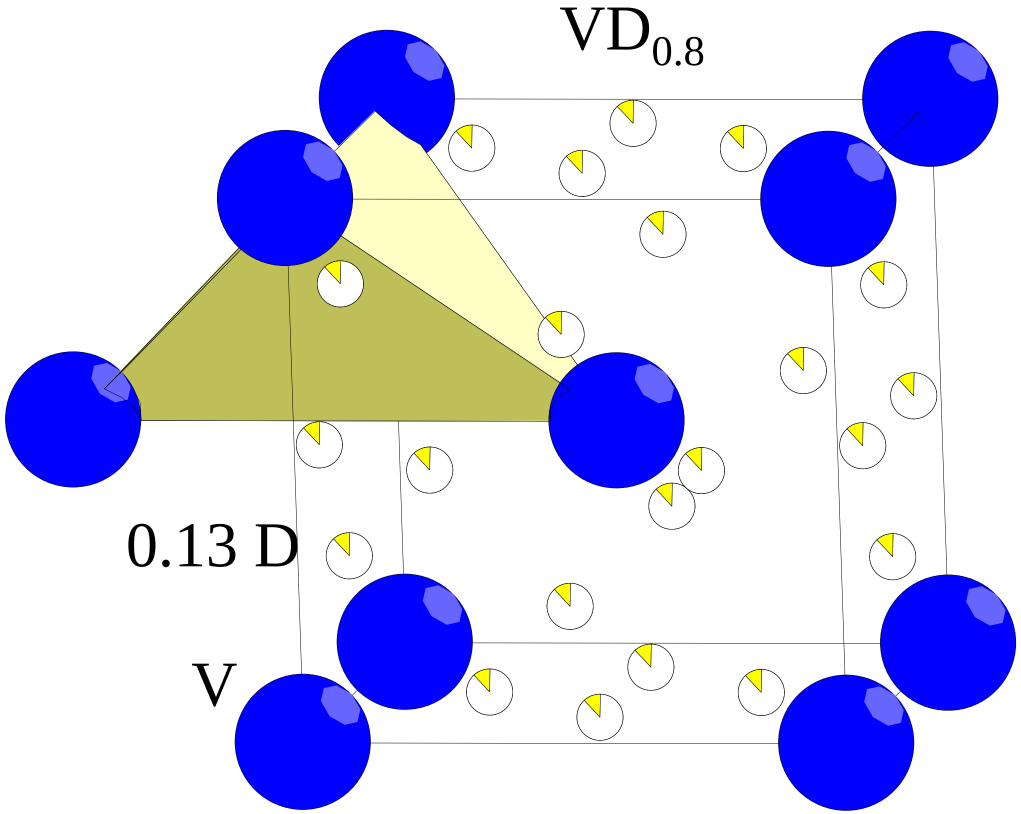

Question we can answer:

- How do the hydrogen atoms relate to the metal atoms?

The average picture of a metal hydride

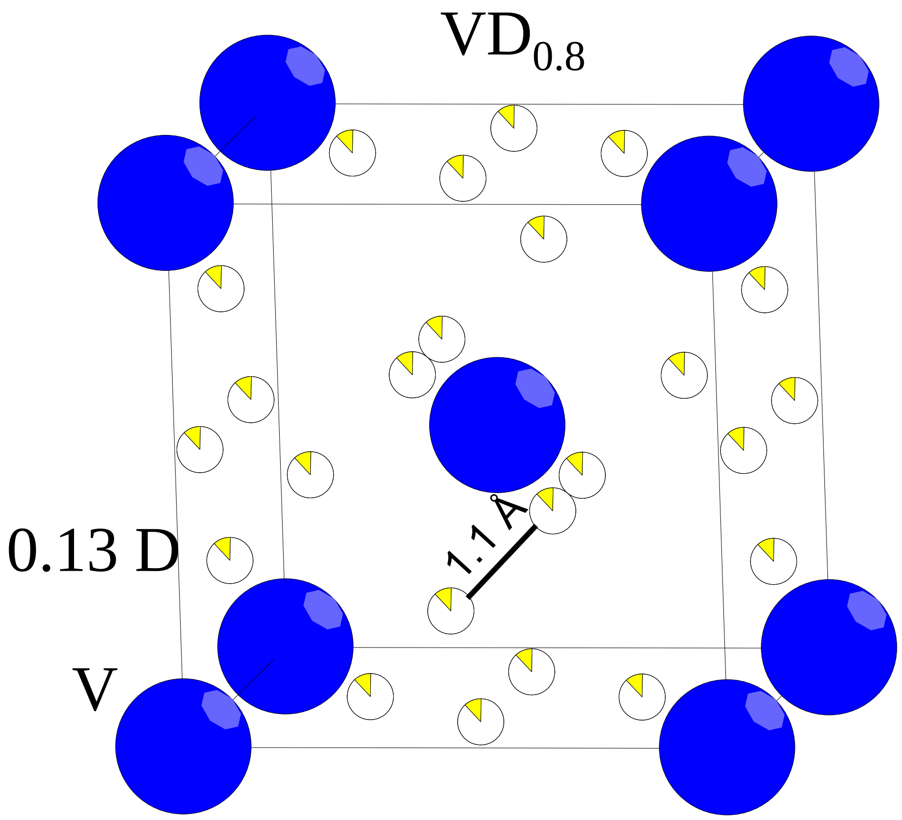

Question we cannot answer:

- What is the shortest distance between the hydrogen atoms?

The ”solution”

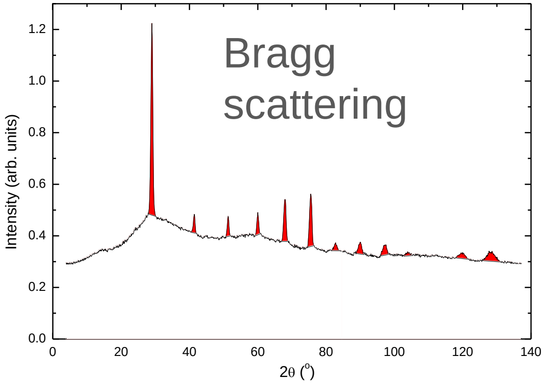

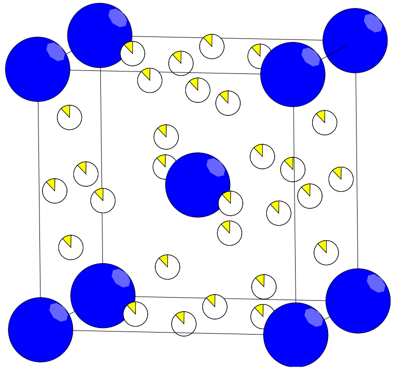

H-H = ??

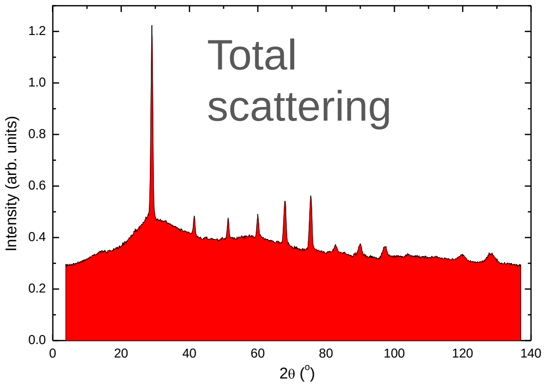

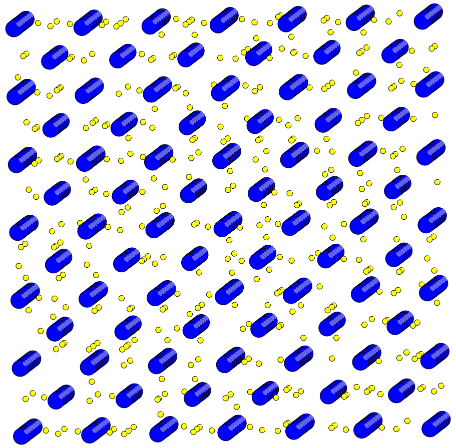

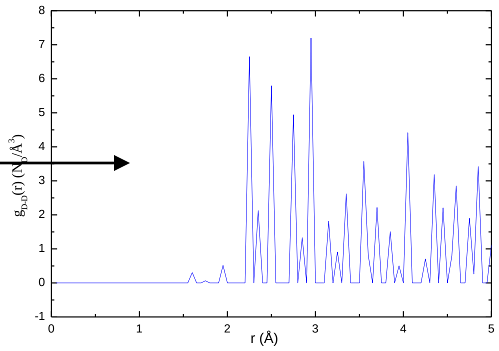

Total scattering

$$S(Q) = \frac{|F(Q)|^2}{N}$$

the structure function

Q = 4π sin(θ)/λ

$$G(r) = \int_Q S(Q)\ e^{-iQ\cdot r} dQ$$

the pair distribution function (PDF)

$$= \sum_{j,k=1}^{M} c_j c_k f_j f_k \cdot g_{j-k}(r)$$

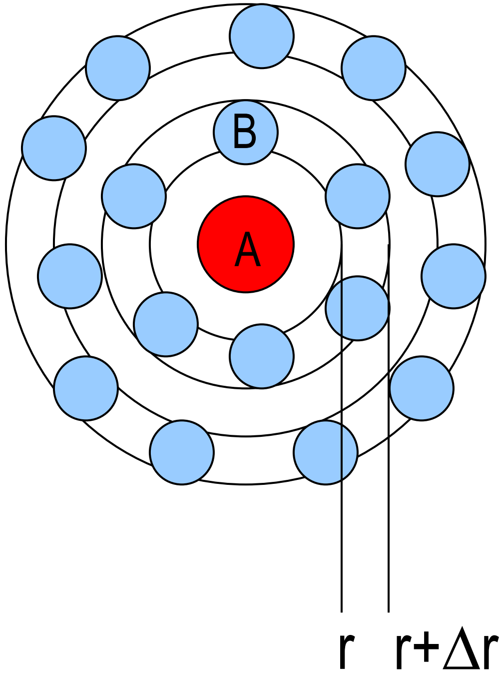

Partial PDF

$$g_{A-B}(r) = \frac{\rho_B(r)}{\rho_B^{overall}}$$

Total scattering

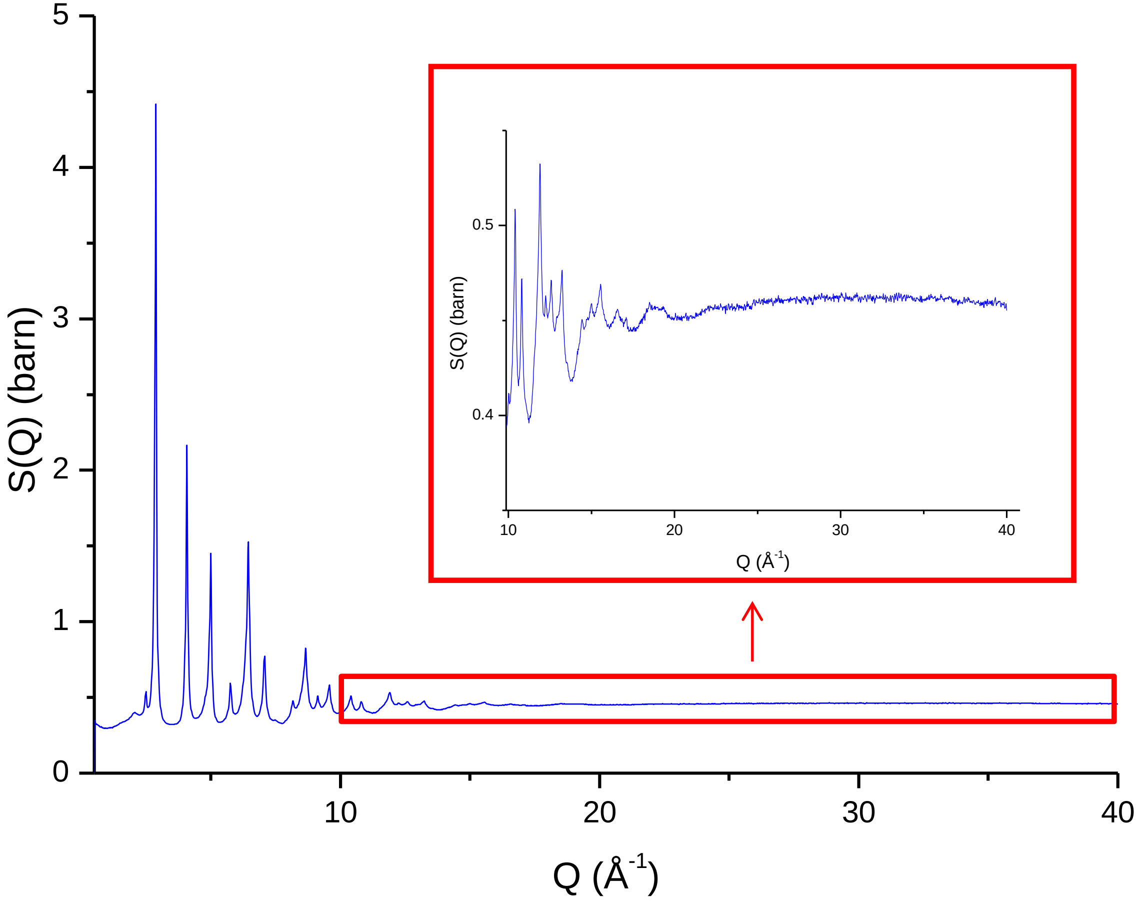

Total scattering

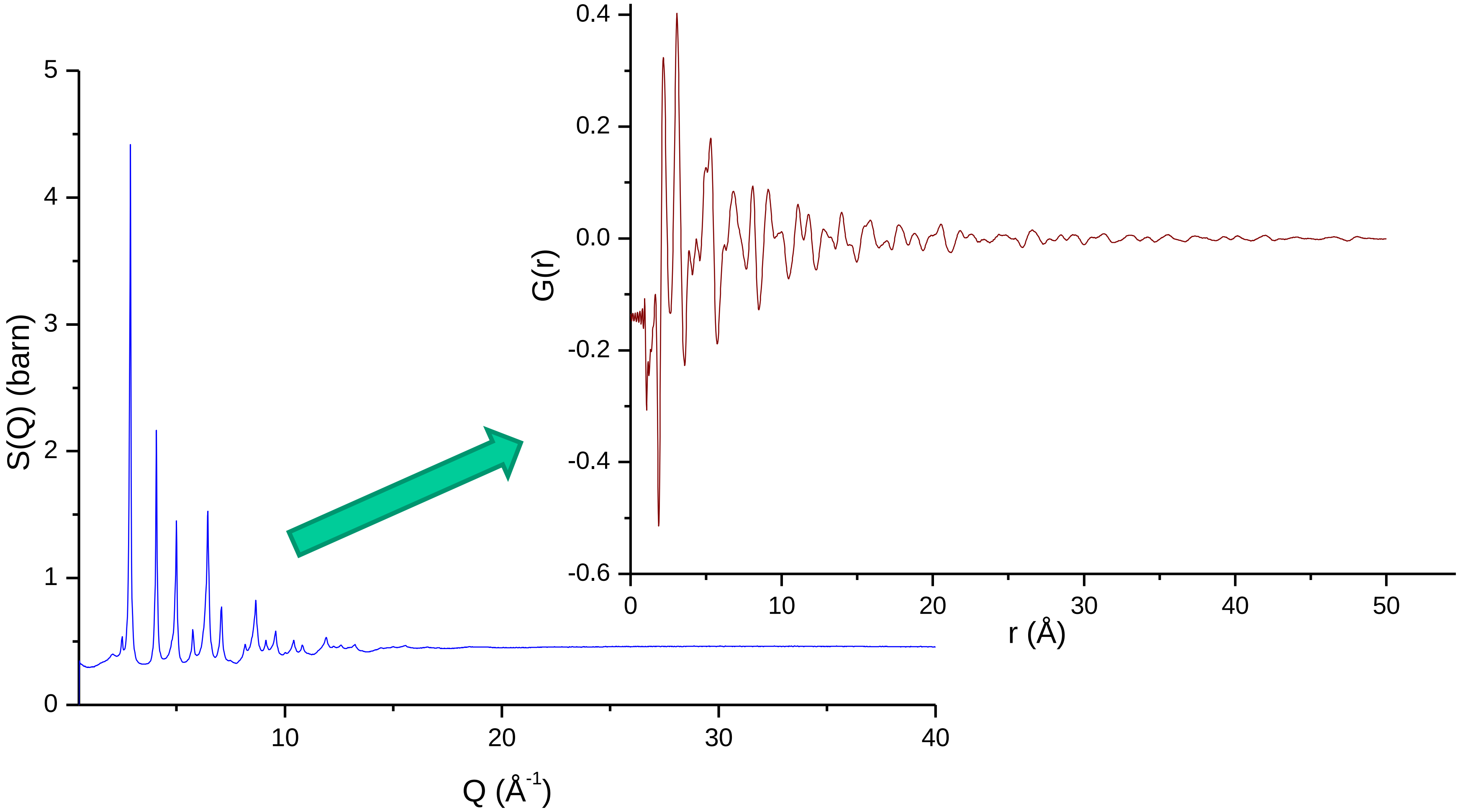

Reverse Monte Carlo (RMC)

Make a large structure model

↓

Calculate the scattering intensity from the model, $I^{Calc}(Q)$

↓

Calculate the agreement with the experimental data

$$\chi^2 = \sum_{i=1}^{m} \frac{(I^{Calc}(Q_i) - I^{Exp}(Q_i))^2}{\sigma(Q_i)}$$

↓

Move one atom at random

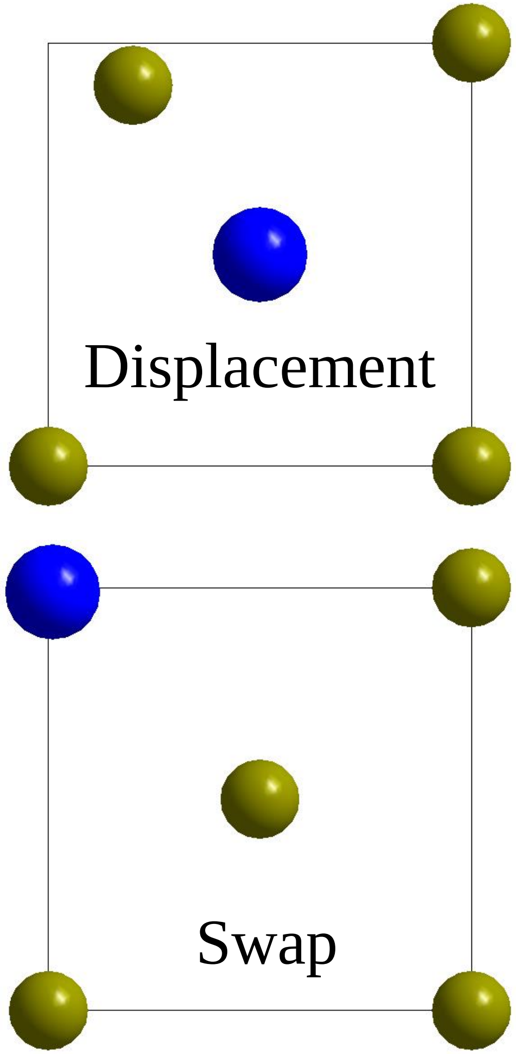

Reverse Monte Carlo (RMC)

Make a large structure model

↓

Calculate the scattering intensity from the model, $I^{Calc}(Q)$

↓

Calculate the agreement with the experimental data

$$\chi^2 = \sum_{i=1}^{m} \frac{(I^{Calc}(Q_i) - I^{Exp}(Q_i))^2}{\sigma(Q_i)}$$

↓

Move one atom at random ←

↓

Calculate the scattering from the new configuration cell, and the new χ^2 →

If $\chi^2_{old} > \chi^2_{new}$ then the new configuration cell is accepted.

If $\chi^2_{old} < \chi^2_{new}$ then the new configuration cell is accepted with the probability $e^{-\frac{\chi^2_{new} - \chi^2_{old}}{2}}$

Motivation

"Hydrogen atoms in metallic hydrides must be separated by at least 2 Å"

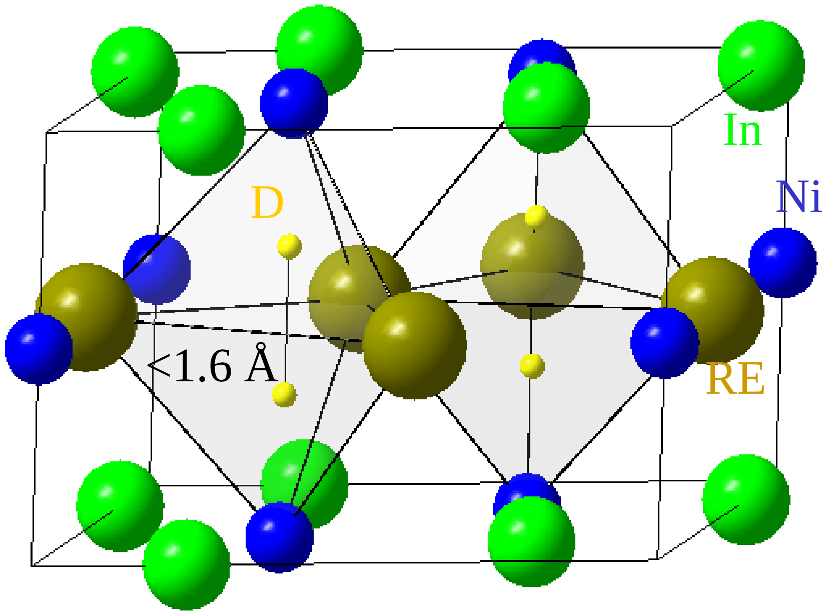

Credible violations found in $RENiInD_{1.33}$

V. A. Yartys, R. V. Denys, B. C. Hauback, H. Fjellvåg, et al., J. Alloys Comp. 330-332 (2002) 132-140.

A model system – $VD_{0.8}$

- simple structure
- "mono-component"
- well-studied

U. Knell, H. Wipf, et al., Journal of Physics: Condensed Matter 6 (1994) 1461-1471.

M. Pionke, W. Schweika, et al., Physica B 213-214 (1995) 567-569.

Y. Sugizaki, S. Yamaguchi, J. Alloys Comp. 231 (1995) 126-131.

Tetrahedral sites 13% occupied

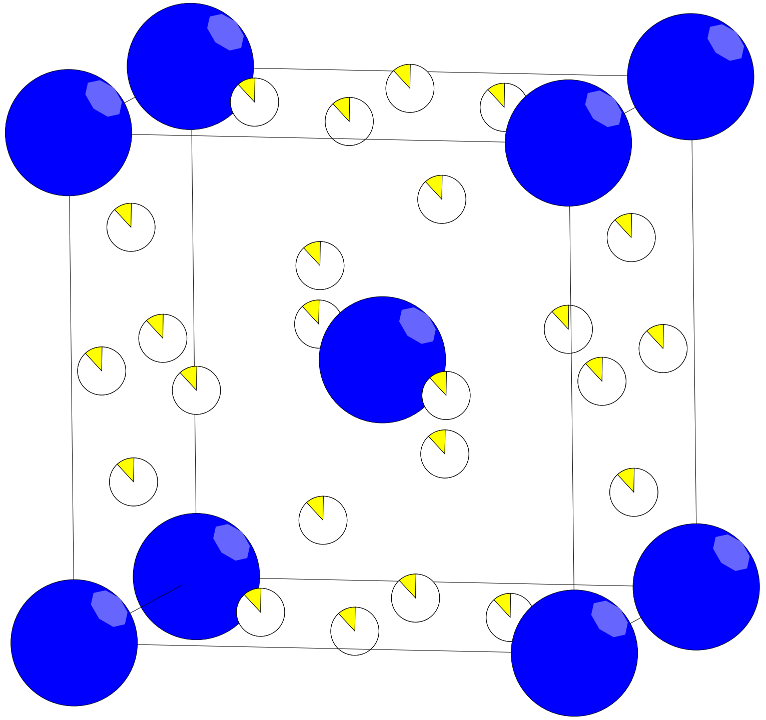

Model from Rietveld refinement

Total scattering measurement

SLAD @ R2, Studsvik, Sweden

4 measurements:
- sample in vanadium can
- empty vanadium can
- empty instrument
- vanadium rod

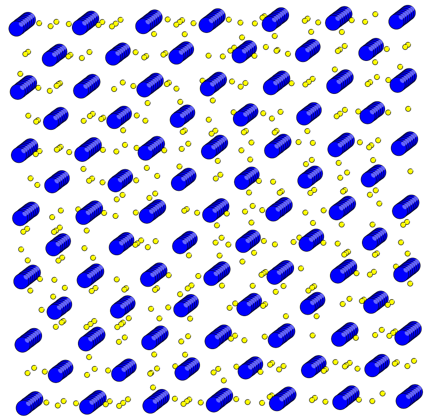

RMC model:

6x6x6 unit cells

432 V atoms

333 D atoms

3456 “vacancies”

Program *CORRECT*
- instrumental background
- absorption
- multiple scattering
- normalization

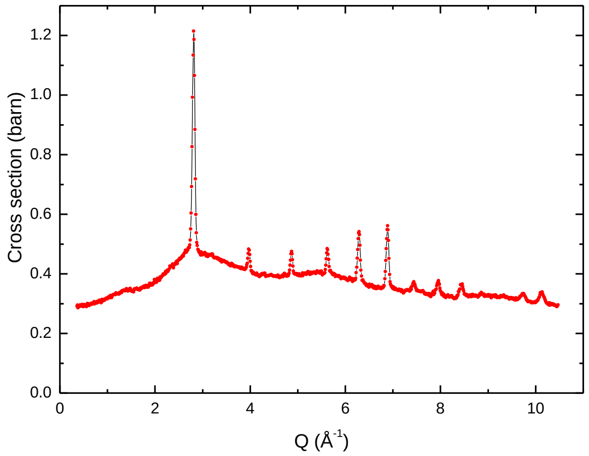

RMC modeling of $VD_{0.8}$

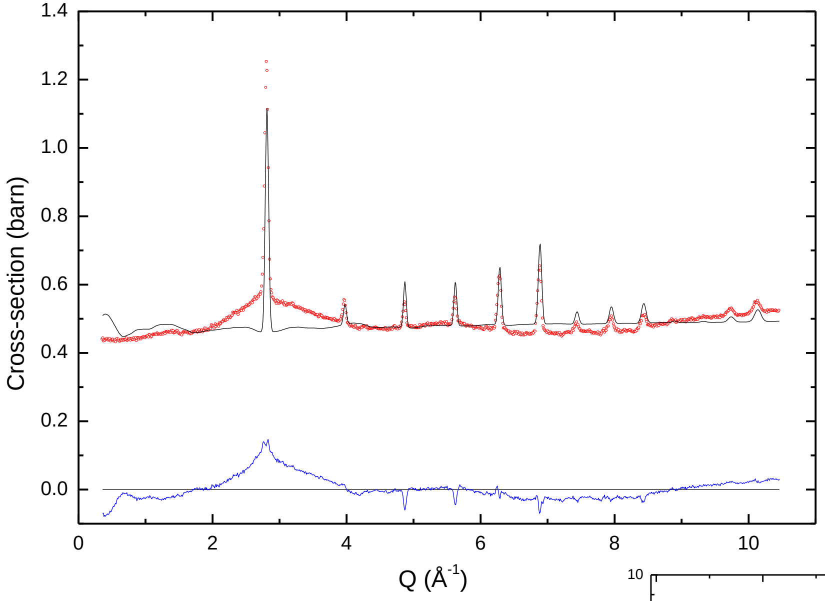

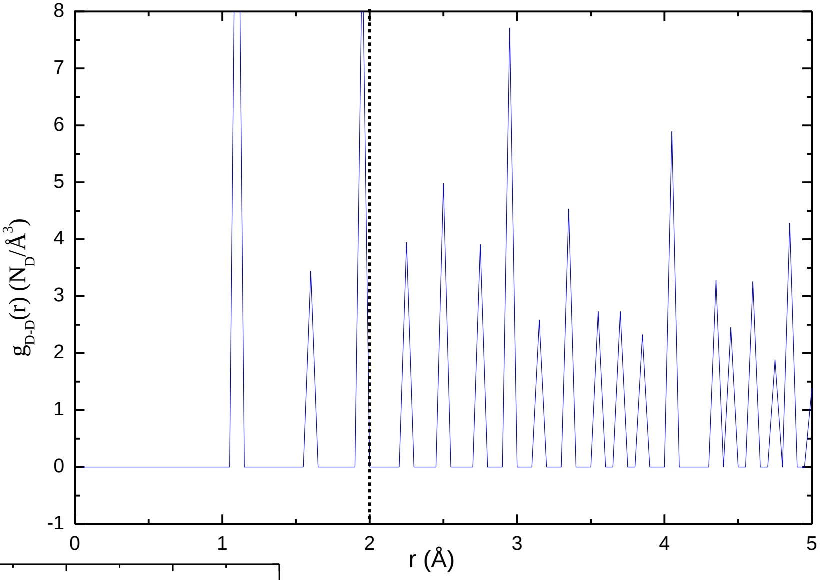

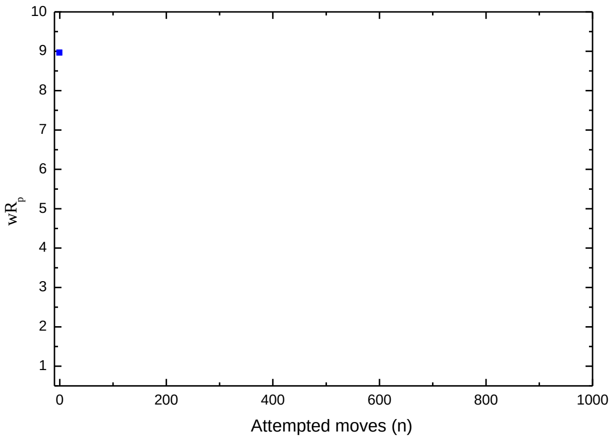

M. H. Sørby, A. Mellergård, R. Delaplane, A. Wannberg, B. C. Hauback, H. Fjellvåg, J. Alloys Comp. 363 (2004) 209-216.

RMC modeling of $VD_{0.8}$

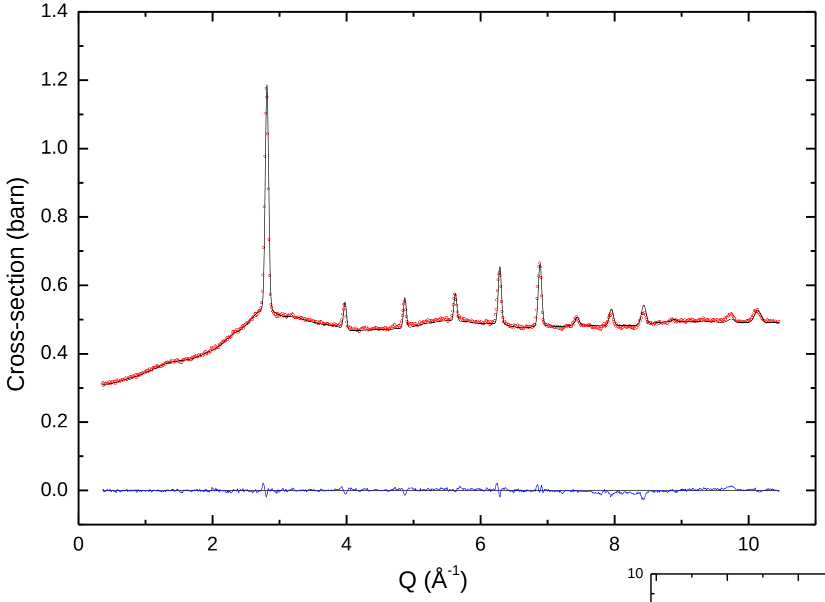

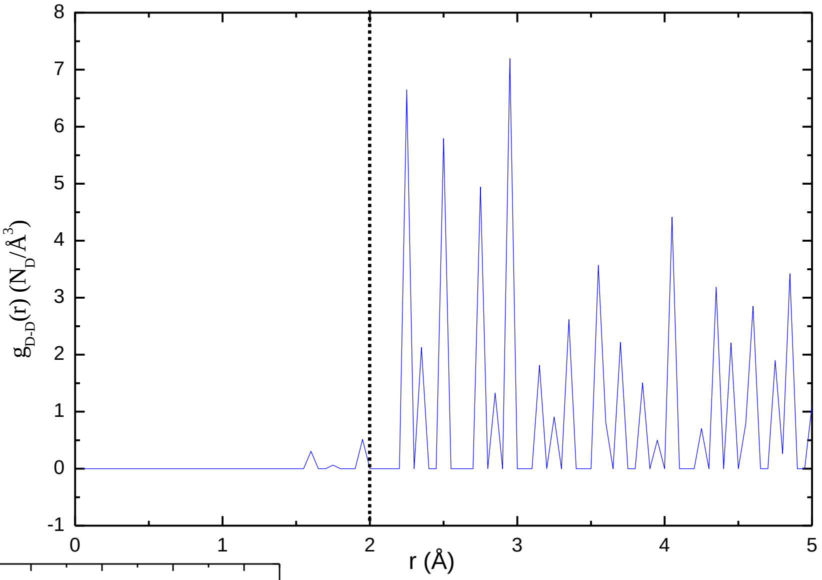

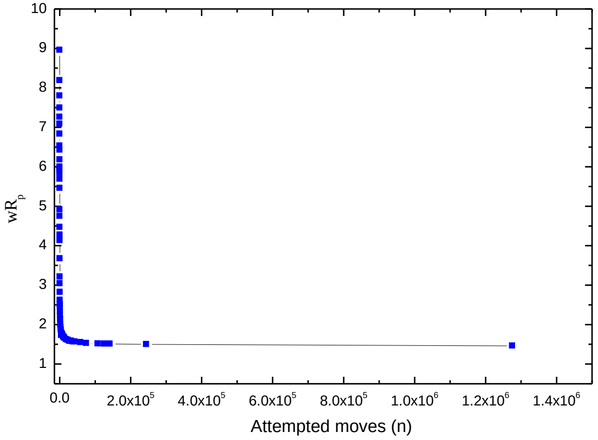

M. H. Sørby, A. Mellergård, R. Delaplane, A. Wannberg, B. C. Hauback, H. Fjellvåg, J. Alloys Comp. 363 (2004) 209-216.

RMC results

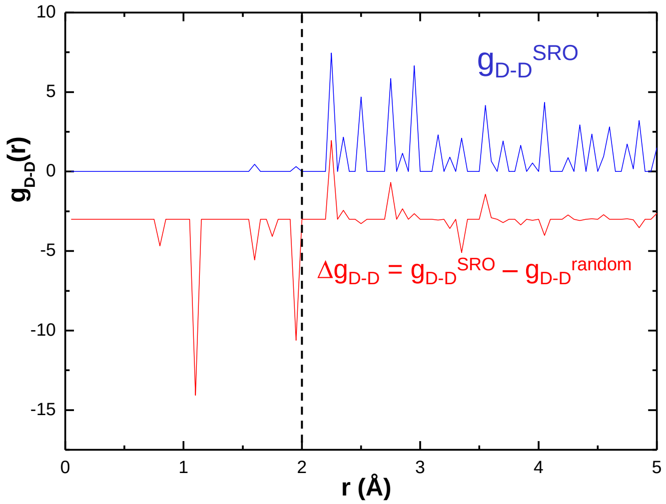

$VD_{0.8}$

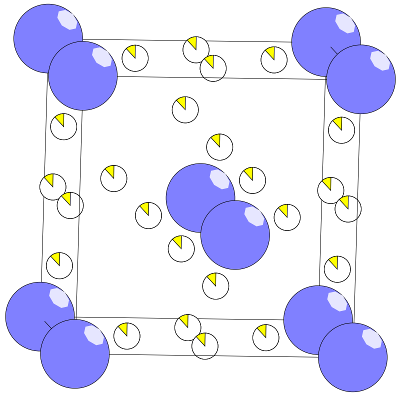

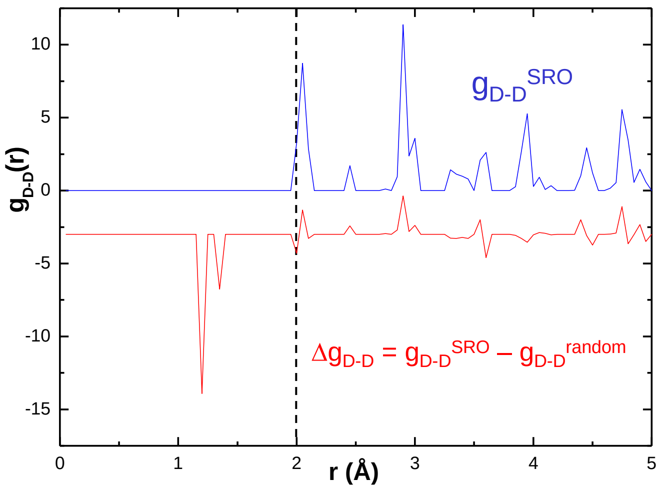

$ZrCr_2D_4$

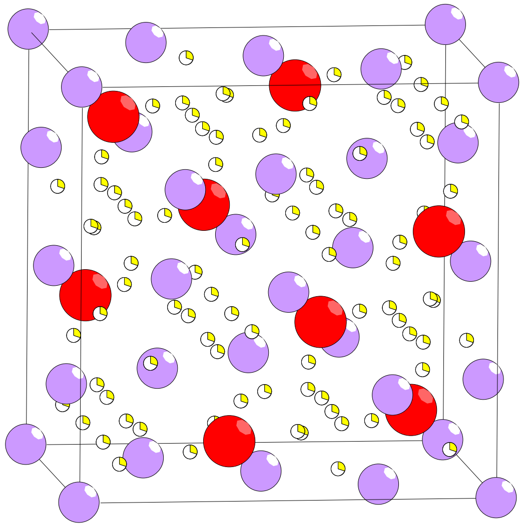

M. H. Sørby, A. Mellergård, R. Delaplane, A. Wannberg, B. C. Hauback, H. Fjellvåg, J. Alloys Comp. 363 (2004) 209-216.

M. H. Sørby, A. Mellergard, B. C. Hauback , H. Fjellvåg, and R. Delaplane, J. Alloys Comp. 459, 225 (2008).

Short-range order vs. long-range order

$VD_{0.8}$

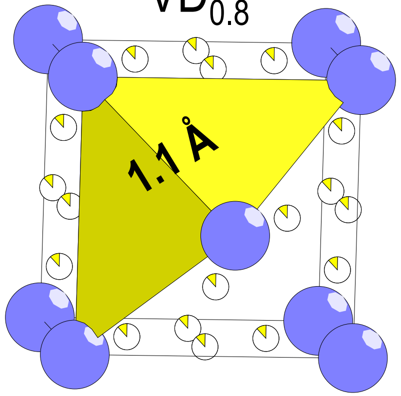

$ZrCr_2D_4$

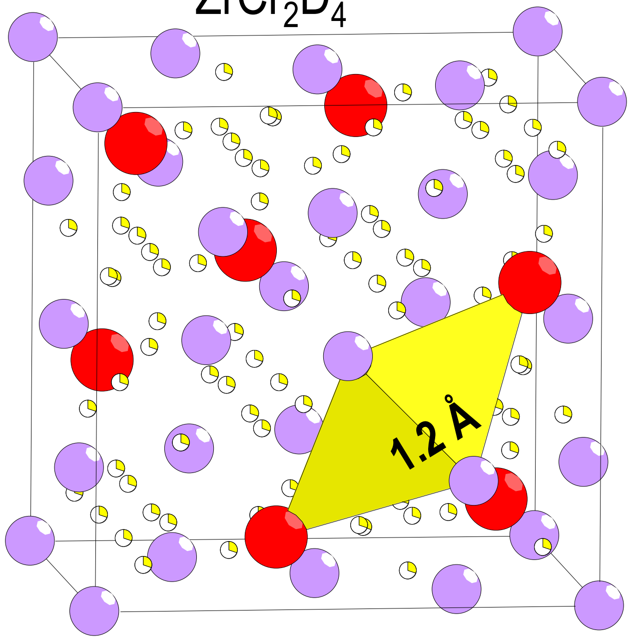

Short-range order vs. long-range order

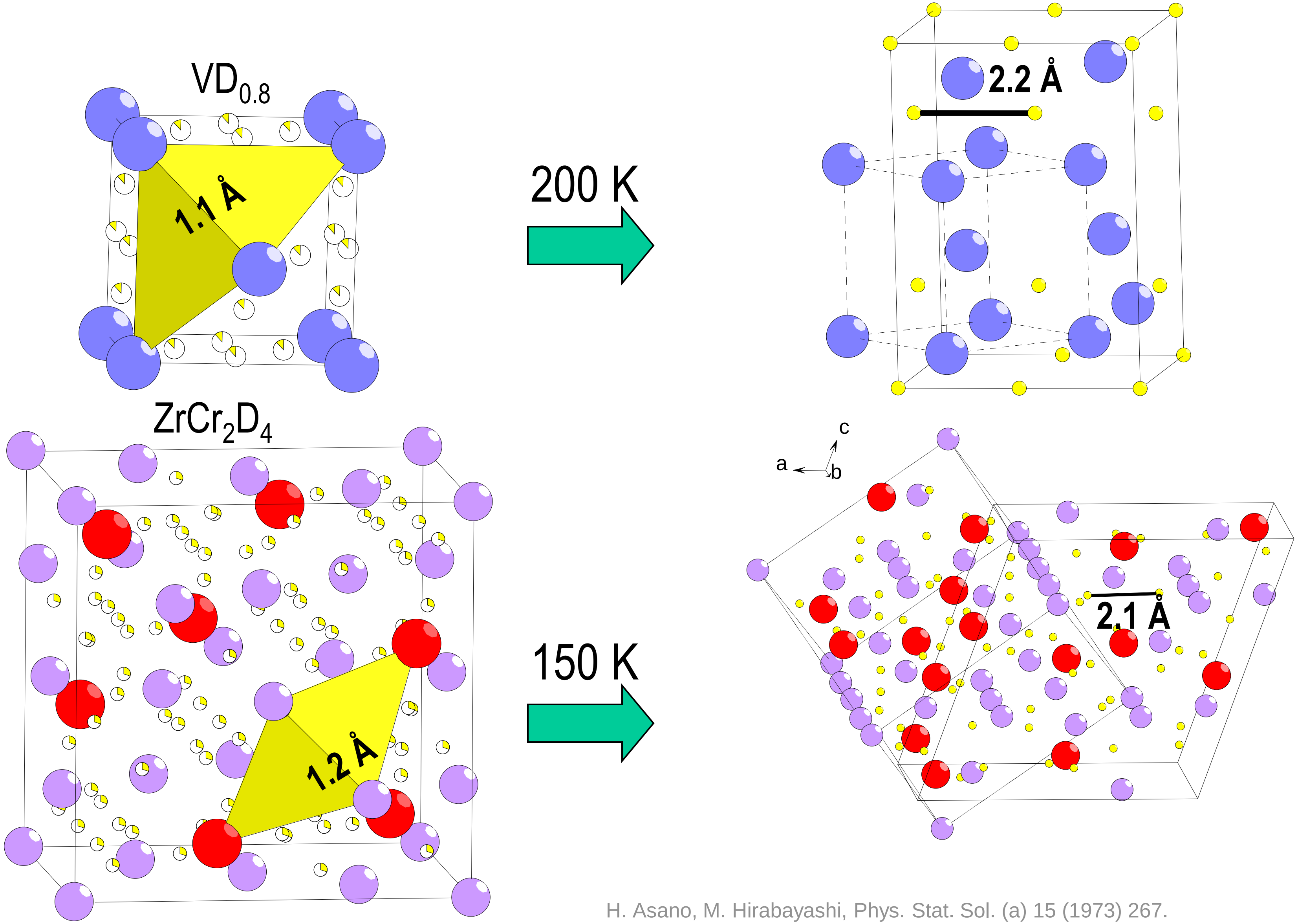

H. Asano, M. Hirabayashi, Phys. Stat. Sol. (a) 15 (1973) 267.
H. Kohlmann, F. Fauth, K. Yvon, J. Alloys Comp. 285 (1999) 204-211.

Short-range order vs. long-range order

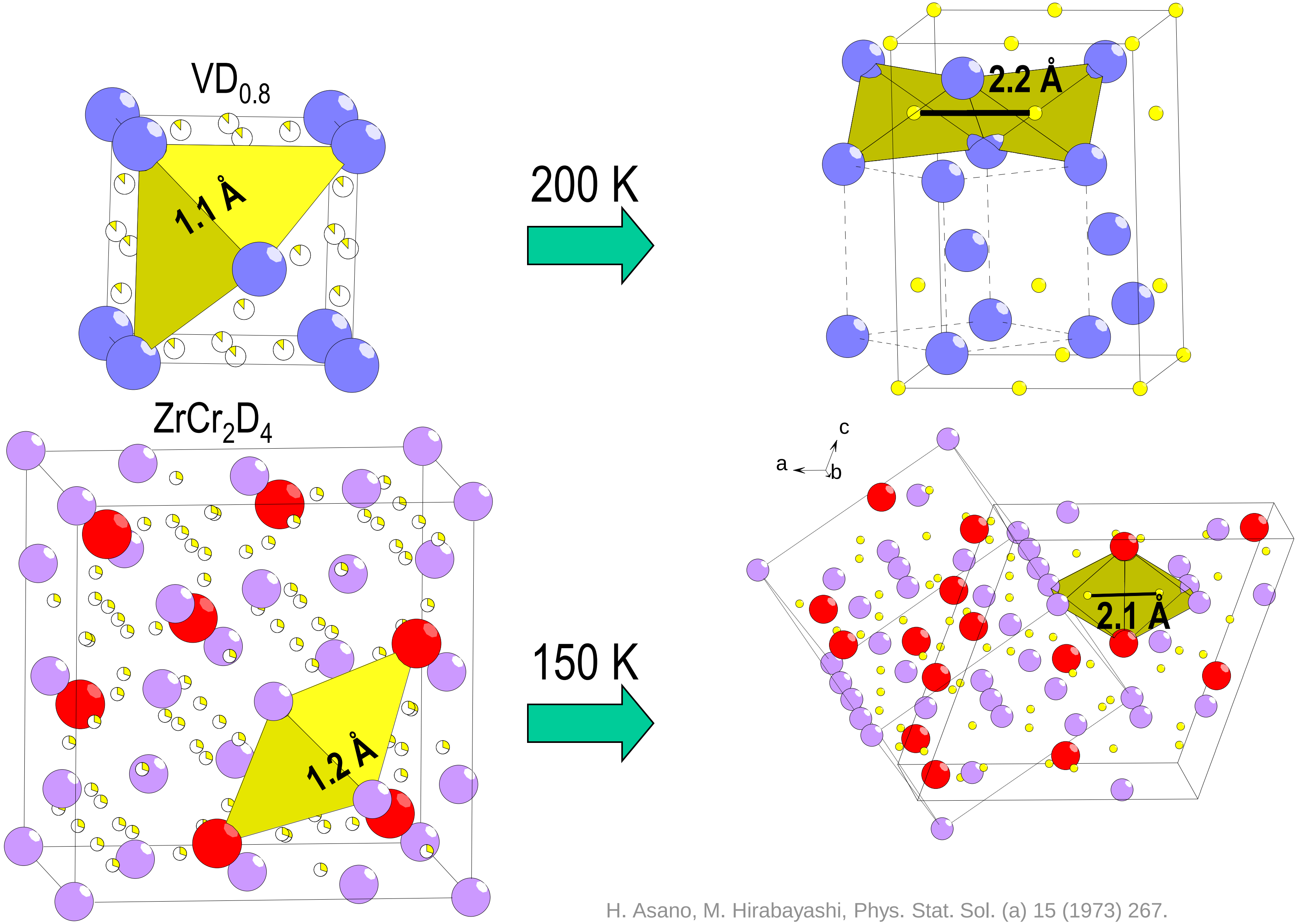

H. Asano, M. Hirabayashi, Phys. Stat. Sol. (a) 15 (1973) 267.
H. Kohlmann, F. Fauth, K. Yvon, J. Alloys Comp. 285 (1999) 204-211.

Short-range order vs. long-range order

Disordered $VD_{0.8}$ (RT) with displacive moves

Ordered $VD_{0.75}$ (taken form literature)

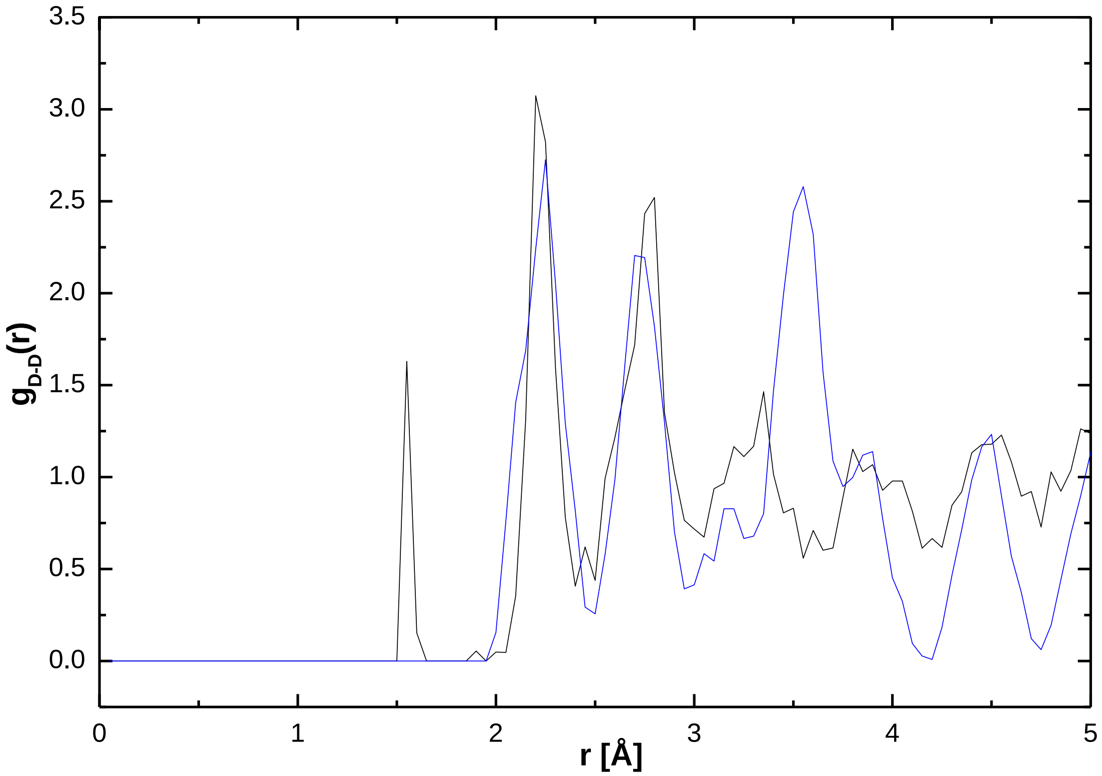

M. H. Sørby, A. Mellergård, R. Delaplane, A. Wannberg, B. C. Hauback, H. Fjellvåg, J. Alloys Comp. 363 (2004) 209-216.

Short-range order vs. long-range order

Disordered $ZrCr_2D_4$ (RT) from RMC

Ordered $ZrCr_2D_4$ (150K) from RMC

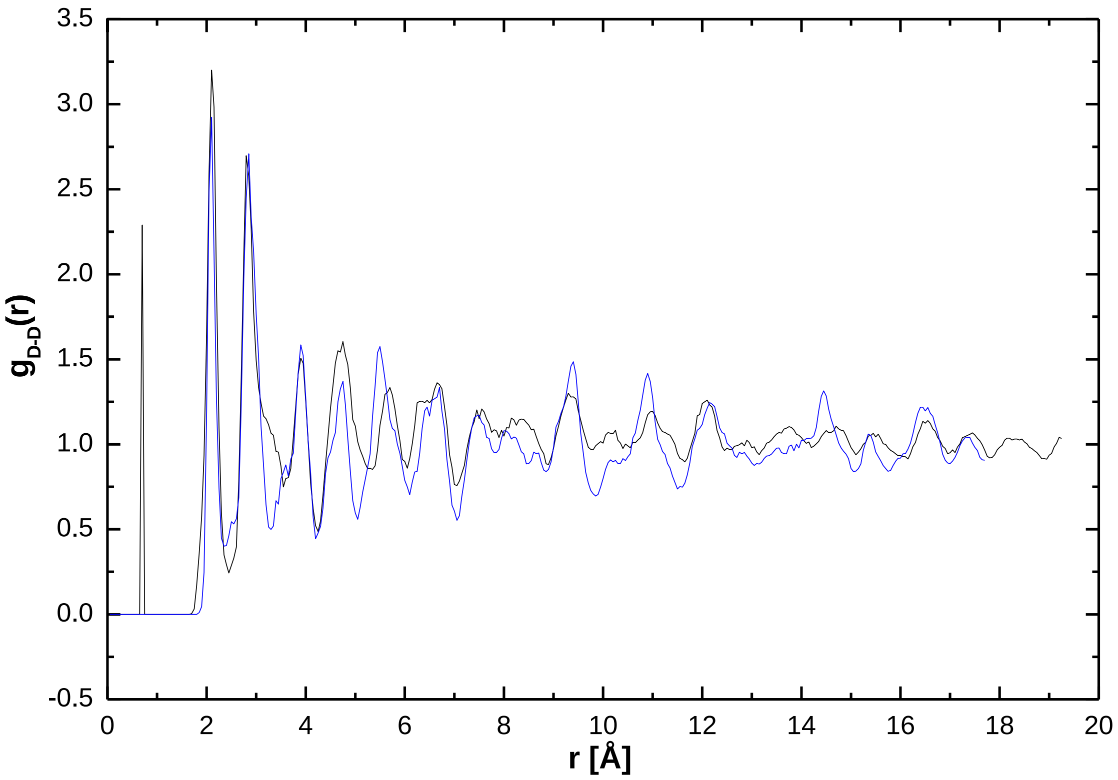

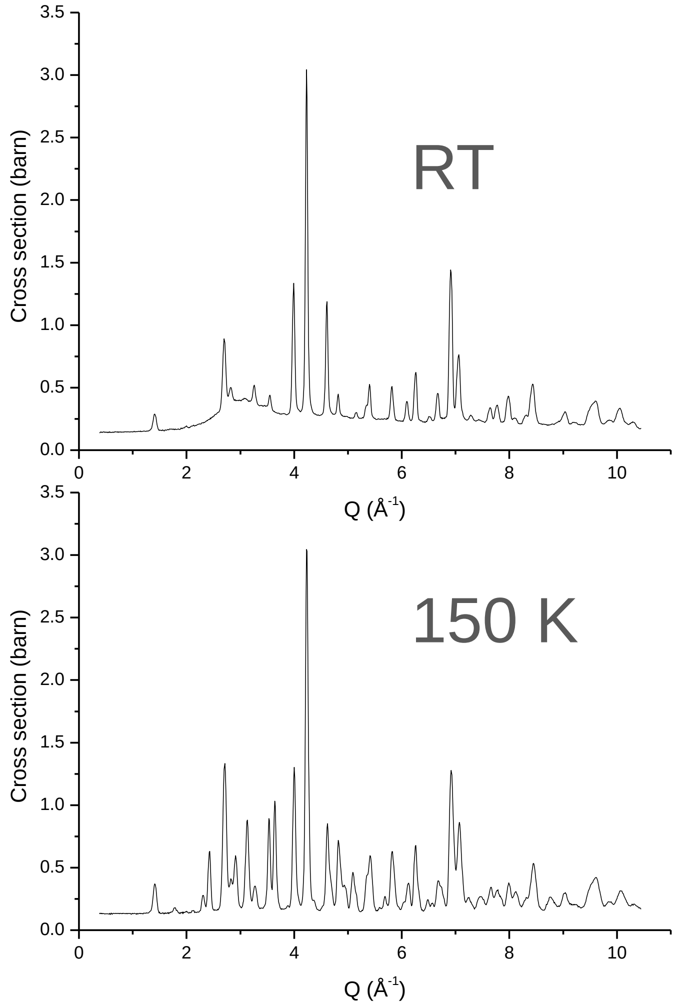

M. H. Sørby, A. Mellergard, B. C. Hauback , H. Fjellvåg, and R. Delaplane, J. Alloys Comp. 459, 225 (2008).

Short-range order vs. long-range order

Disordered $ZrCr_2D_4$ (RT) from RMC

Ordered $ZrCr_2D_4$ (150K) from RMC

$ZrCr_2D_4$ with fully random D distribution

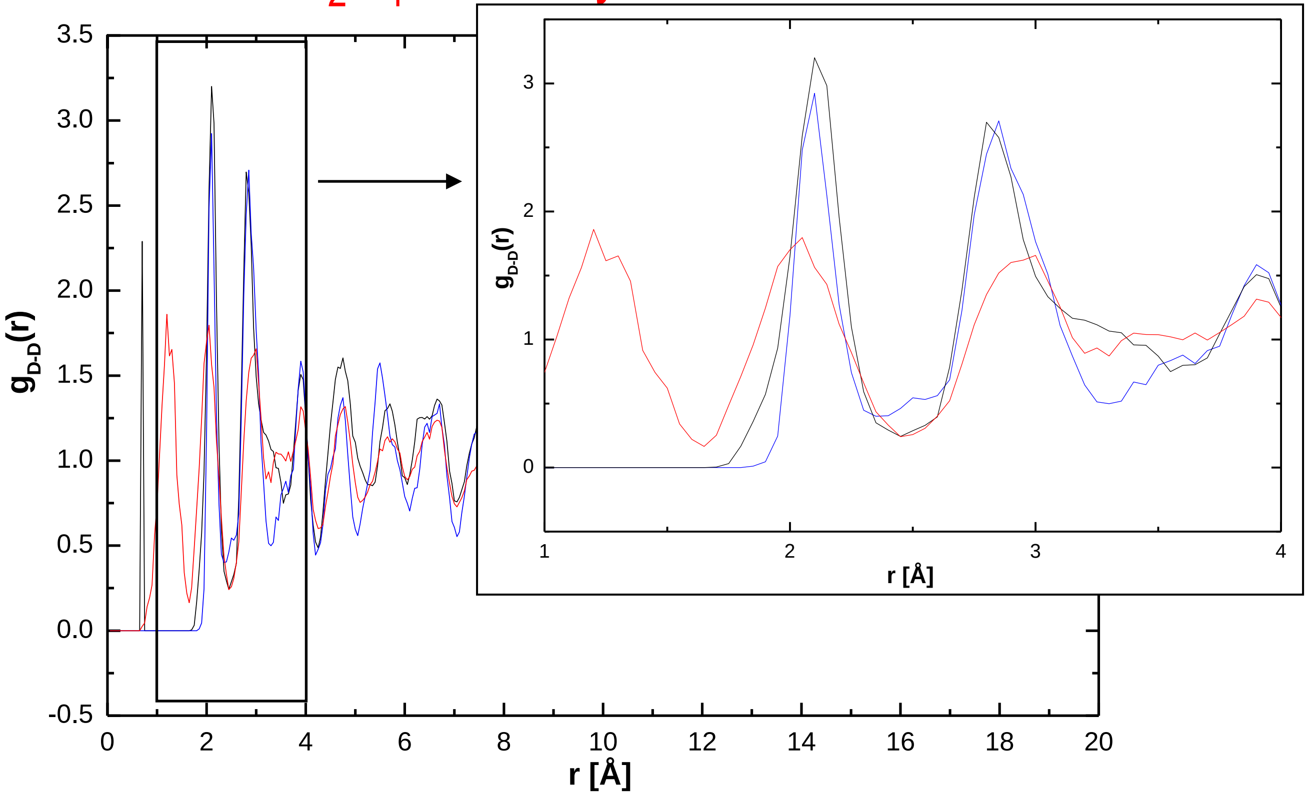

M. H. Sørby, A. Mellergard, B. C. Hauback , H. Fjellvåg, and R. Delaplane, J. Alloys Comp. 459, 225 (2008).

Octahedral deuterium in $VD_{0.8}$

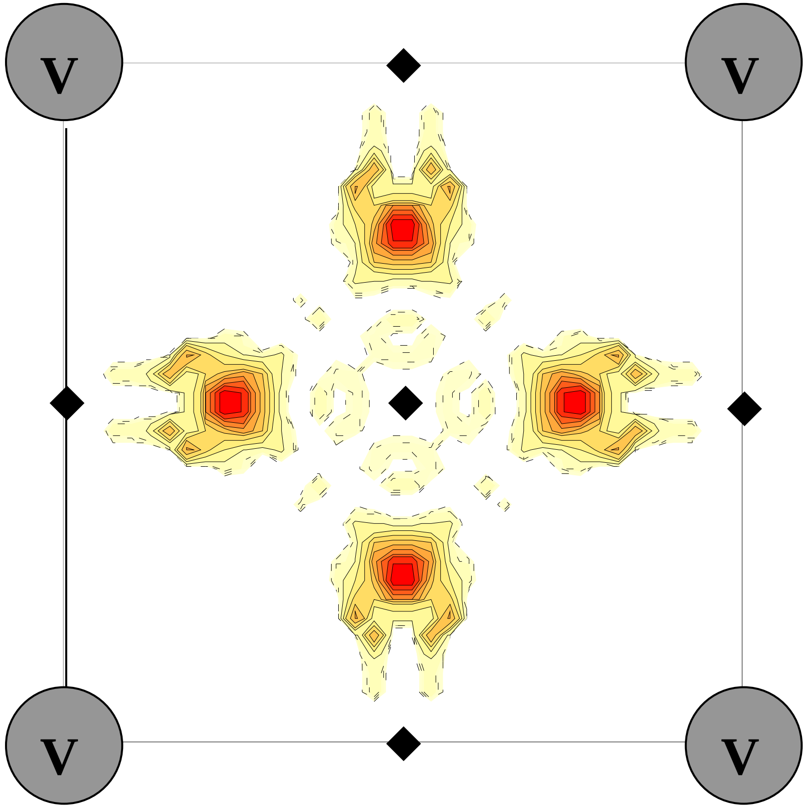

- Rietveld and ”swap-only” RMC: ~6% of D- atoms are in octahedral sites.
- Displacive moves: D-atoms avoid the centra of octahedral sites.

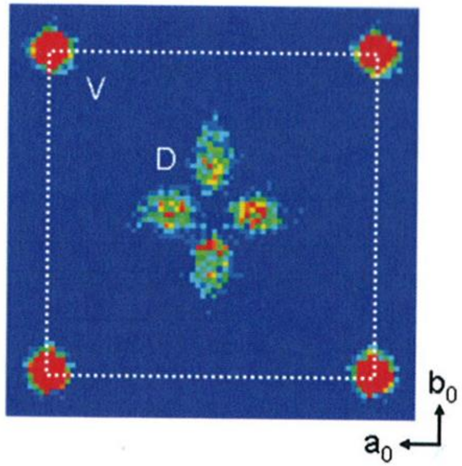

β - V_2D

M. H. Sørby, A. Mellergård, R. Delaplane, A. Wannberg, B. C. Hauback, H. Fjellvåg, J. Alloys Comp. 363 (2004) 209-216.

K. Itoh and T. Fukunaga, Journal of Applied Physics 101 (2007) 123528.

Octahedral deuterium in $VD_{0.8}$

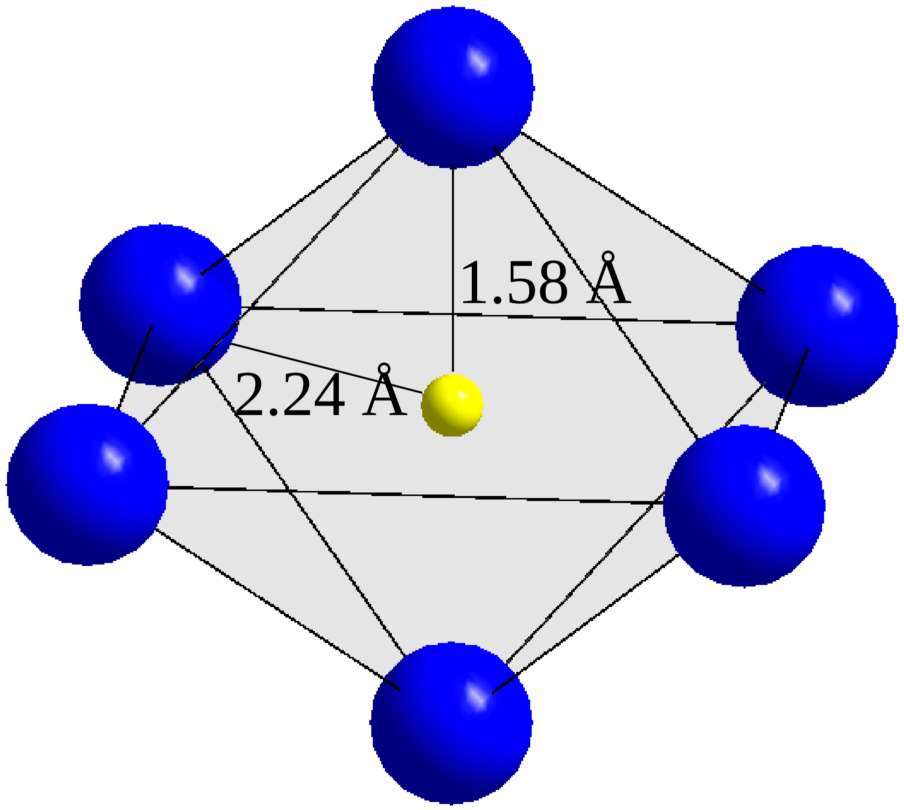

- Rietveld and ”swap-only” RMC: ~6% of D- atoms are in octahedral sites.
- Displacive moves: D-atoms avoid the centra of octahedral sites.

M. H. Sørby, A. Mellergård, R. Delaplane, A. Wannberg, B. C. Hauback, H. Fjellvåg, J. Alloys Comp. 363 (2004) 209-216.

Another case study:

bcc alloys for H storage

Based on the Ti-V svstem

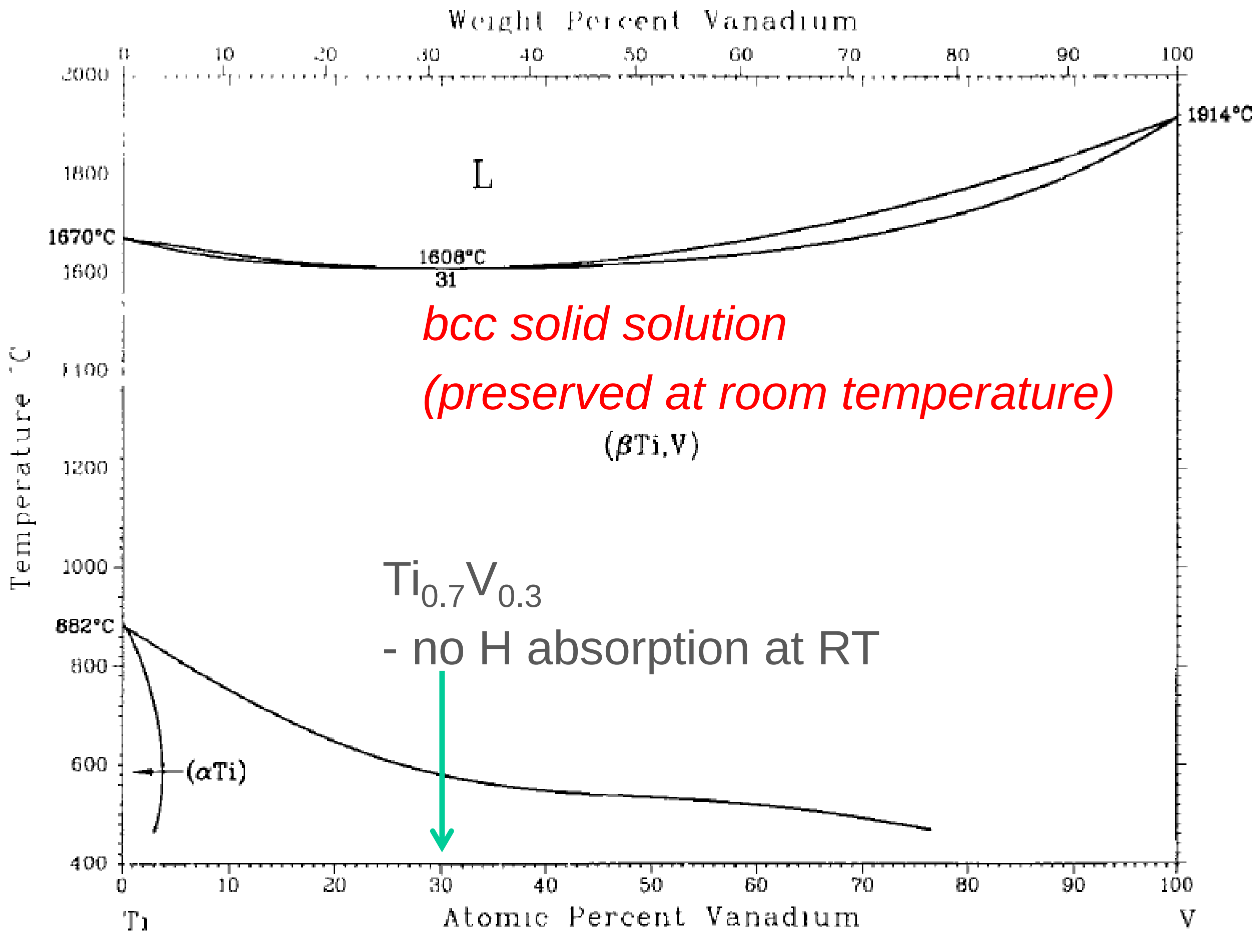

Maeland, A. J., G. G. Libowitz and J. F. Lynch (1984) Journal of the Less-Common Metals **104(2): 361-364.**

bcc alloys for H storage

Based on the Ti-V svstem

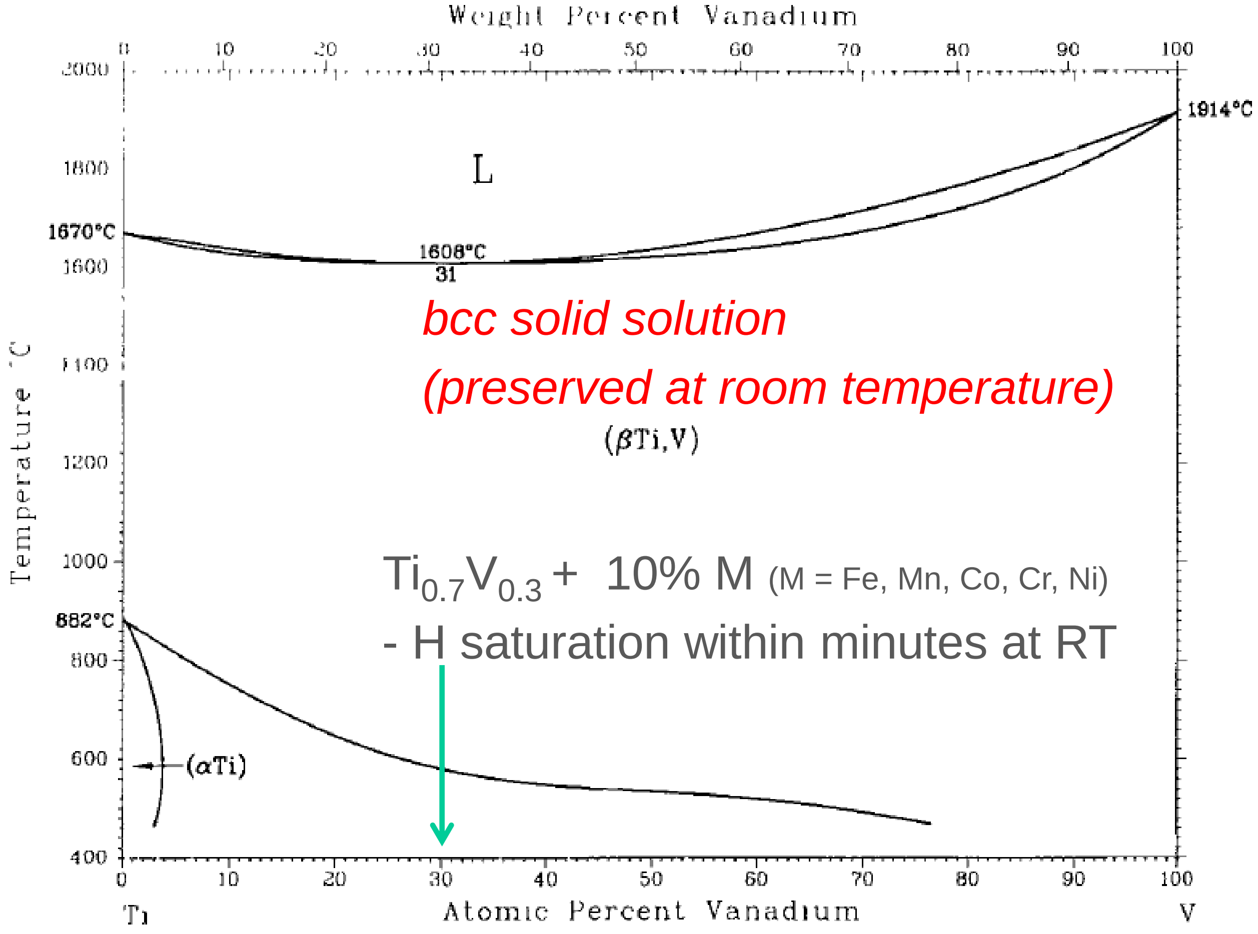

Maeland, A. J., G. G. Libowitz and J. F. Lynch (1984) Journal of the Less-Common Metals **104(2): 361-364.**

bcc alloy hydrides

Based on the Ti-V system

AB_5 (“$LaNi_5$”) hydrides

+ Excellent kinetics

+ Excellent thermodynamics

- Poor H capacity (~1 w%)

MgH_2

+ Good kinetics if catalysed

- High desorption temperature

+ Excellent H capacity (~7.6 w%)

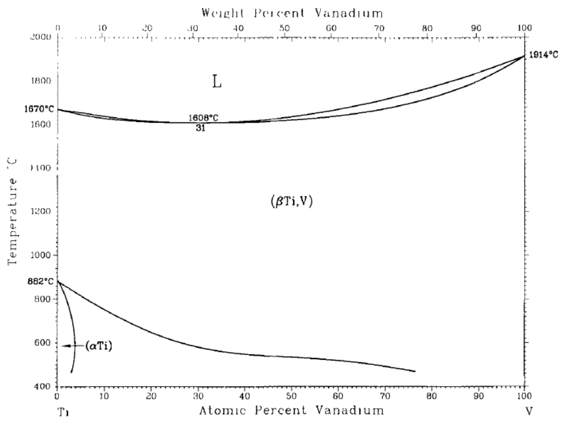

Ti-V-based bcc hydrides

+ Excellent kinetics

+ Excellent thermodynamics

* Decent H capacity (2-3 w%)

Maeland, A. J., G. G. Libowitz and J. F. Lynch (1984) Journal of the Less-Common Metals **104(2): 361-364.**

The challenge of cost

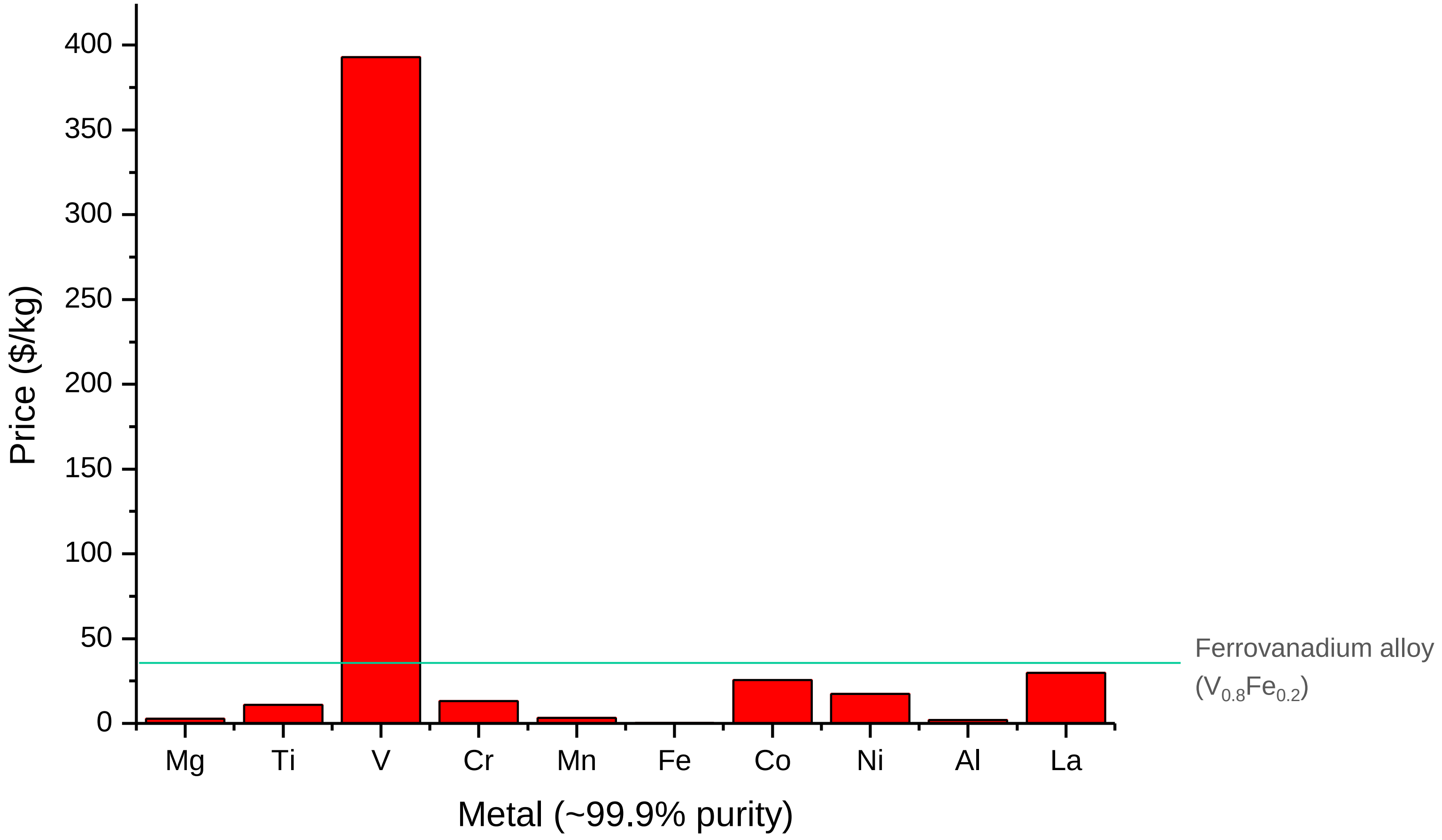

www.metalprices.com

Ferrovanadium-based bcc alloys

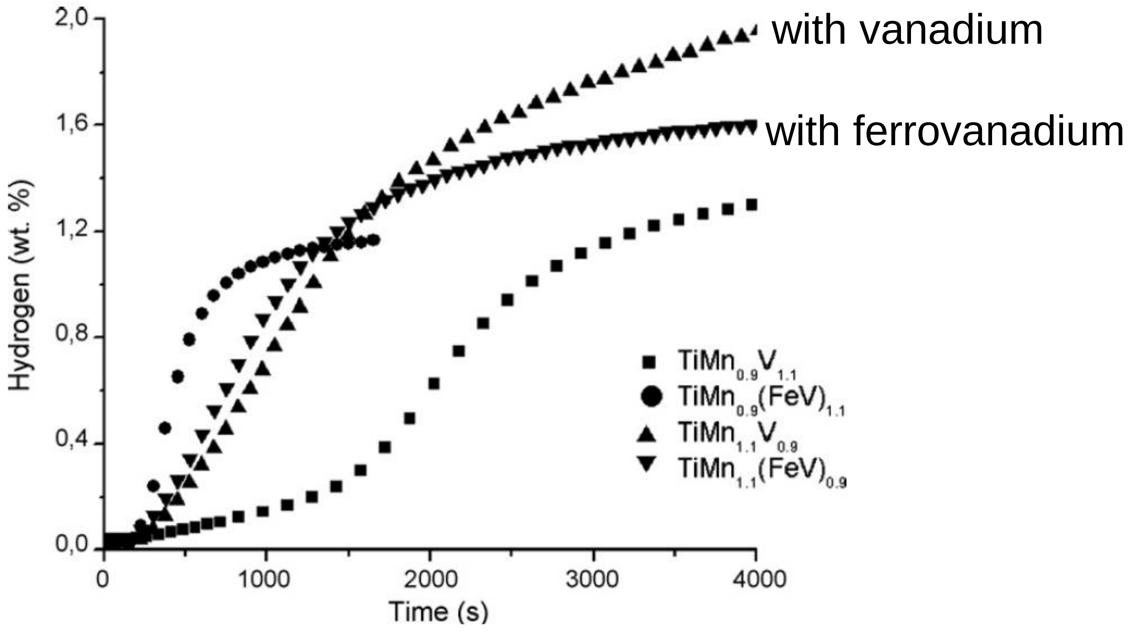

from S.F. Santos, J. Huot, J. Alloys Comp. 480 (2009) 5-8.

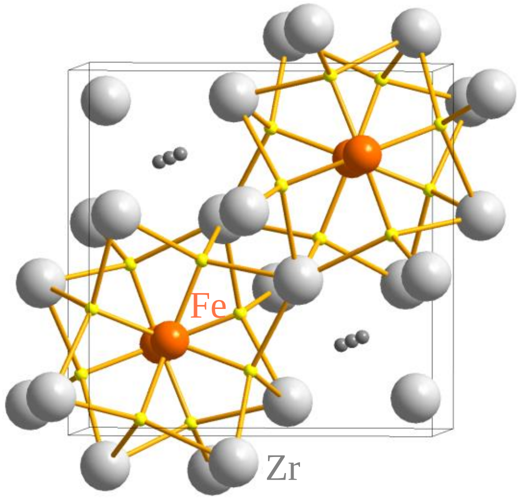

Zr_2FeD_5
80% of D in Zr_3Fe tetrahedra

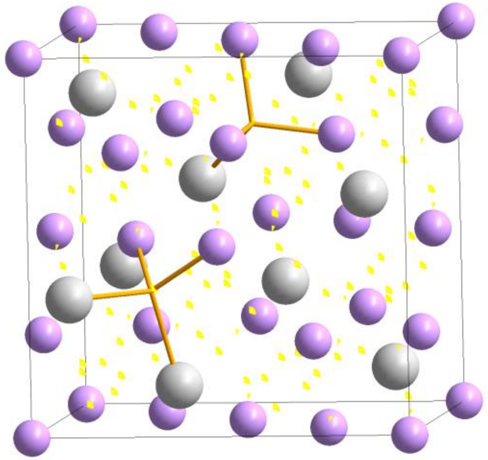

$ZrCrD_4$
90% of D in Zr_2Cr_2 tetrahedra
10% of D in $ZrCr_3$ tetrahedra

Structural reason for the capacity loss?

V.A. Yartys, H. Fjellvåg, I.R. Harris, B.C. Hauback, A.B. Riabov, M.H. Sørby, I.Y. Zavaliy, J. Alloys Comp. 293 (1999) 74-87.

D. Fruchart, A. Rouault, C.B. Shoemaker, D.P. Shoemaker, J. Less-Com. Met. 73 (1980) 363-368.

Crystallography

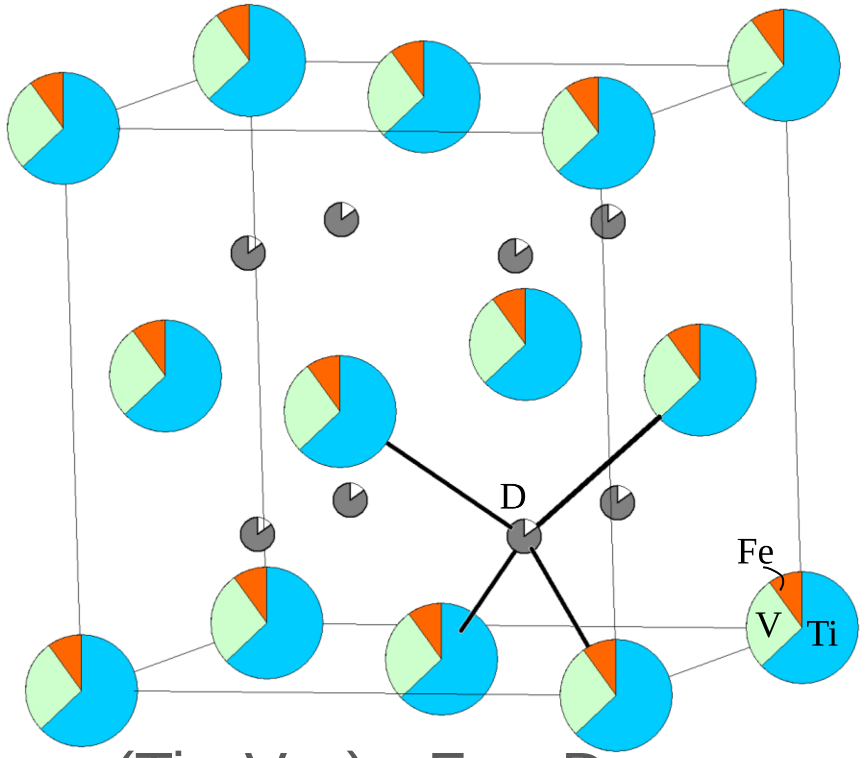

$(Ti_{0.7}V_{0.3})_{0.9}Fe_{0.1}D_{1.7}$

65.6% M_4 tetrahedra
29.2% M_3Fe tetrahedra
4.9% M_2Fe_2 tetrahedra
0.4% MFe_3 tetrahedra
0.01% Fe_4 tetrahedra

99.6 % of sites OK for deuterium?

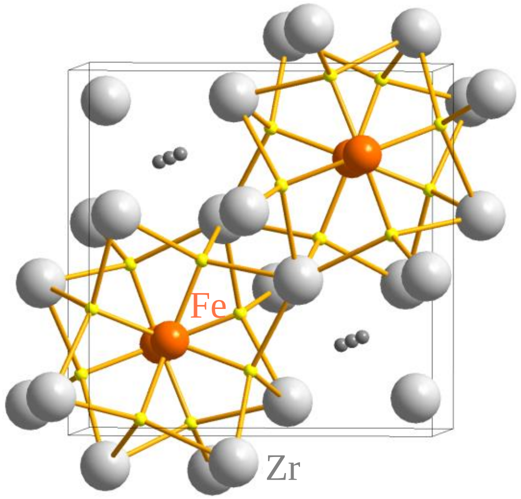

Zr_2FeD_5
80% of D in Zr_3Fe tetrahedra

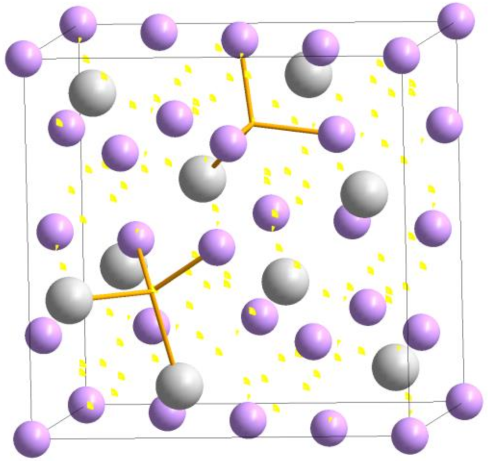

$ZrCrD_4$
90% of D in Zr_2Cr_2 tetrahedra
10% of D in $ZrCr_3$ tetrahedra

V.A. Yartys, H. Fjellvåg, I.R. Harris, B.C. Hauback, A.B. Riabov, M.H. Sørby, I.Y. Zavaliy, J. Alloys Comp. 293 (1999) 74-87.
D. Fruchart, A. Rouault, C.B. Shoemaker, D.P. Shoemaker, J. Less-Com. Met. 73 (1980) 363-368.

Experimental work

Synthesis: Arc melting

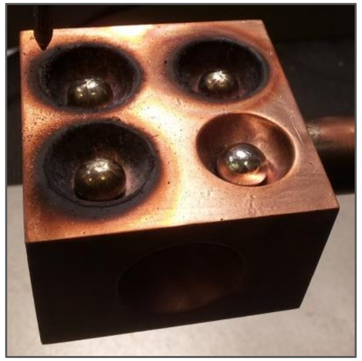

$(Ti_{0.7}V_{0.3})_{0.9}Fe_{0.1}$

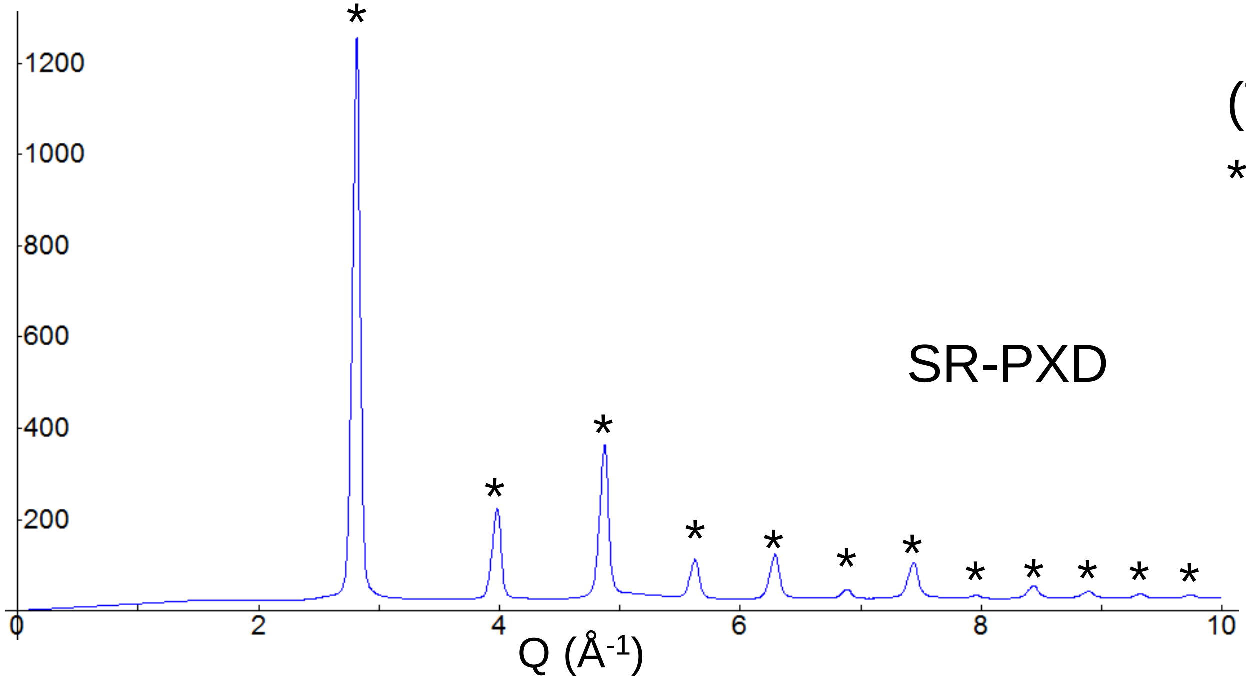

SR-PXD

$(Ti_{0.7}V_{0.3})_{0.9}Fe_{0.1}$

* - bcc

Experimental work

$(Ti_{0.7}V_{0.3})_{0.9}Fe_{0.}$
* - fcc

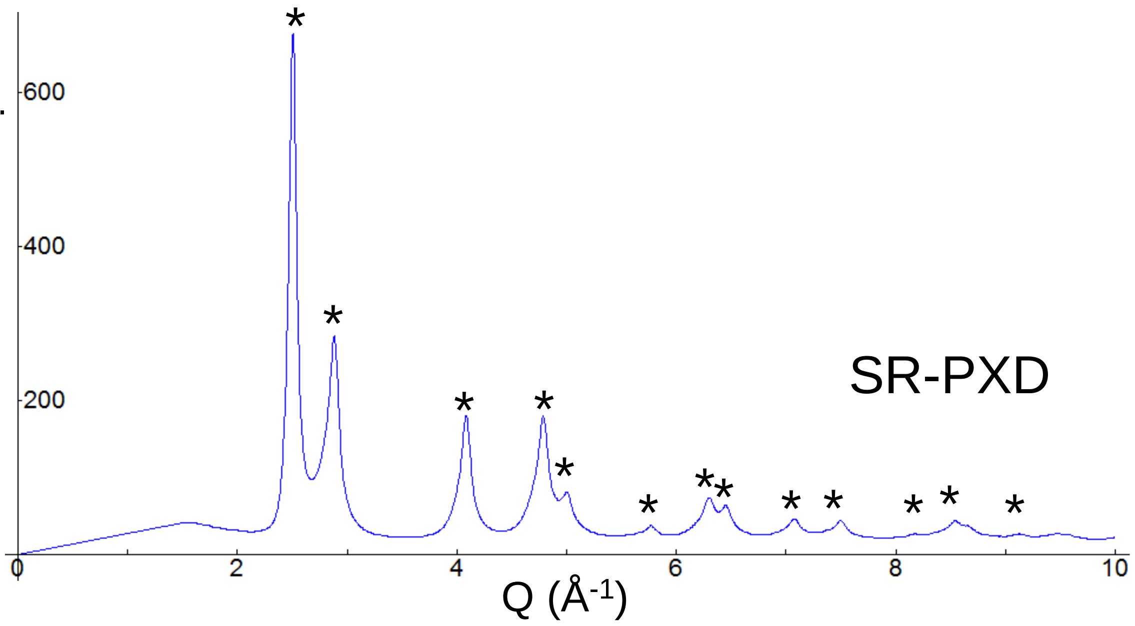

SR-PXD

Synthesis: Deuteration

27 bar D_2 @ 298 K

$(Ti_{0.7}V_{0.3})_{0.9}Fe_{0.1}D_{1.73}$

ISIS, GEM total scattering

Reciprocal space F(Q) → Fourier transform → Real space G(r)

«the PDF»

$$G(\mathbf{r}) = \sum_{j,k} c_j c_k b_j b_k g_{jk}(\mathbf{r}) = FT^{-1}(S(\mathbf{Q}))$$

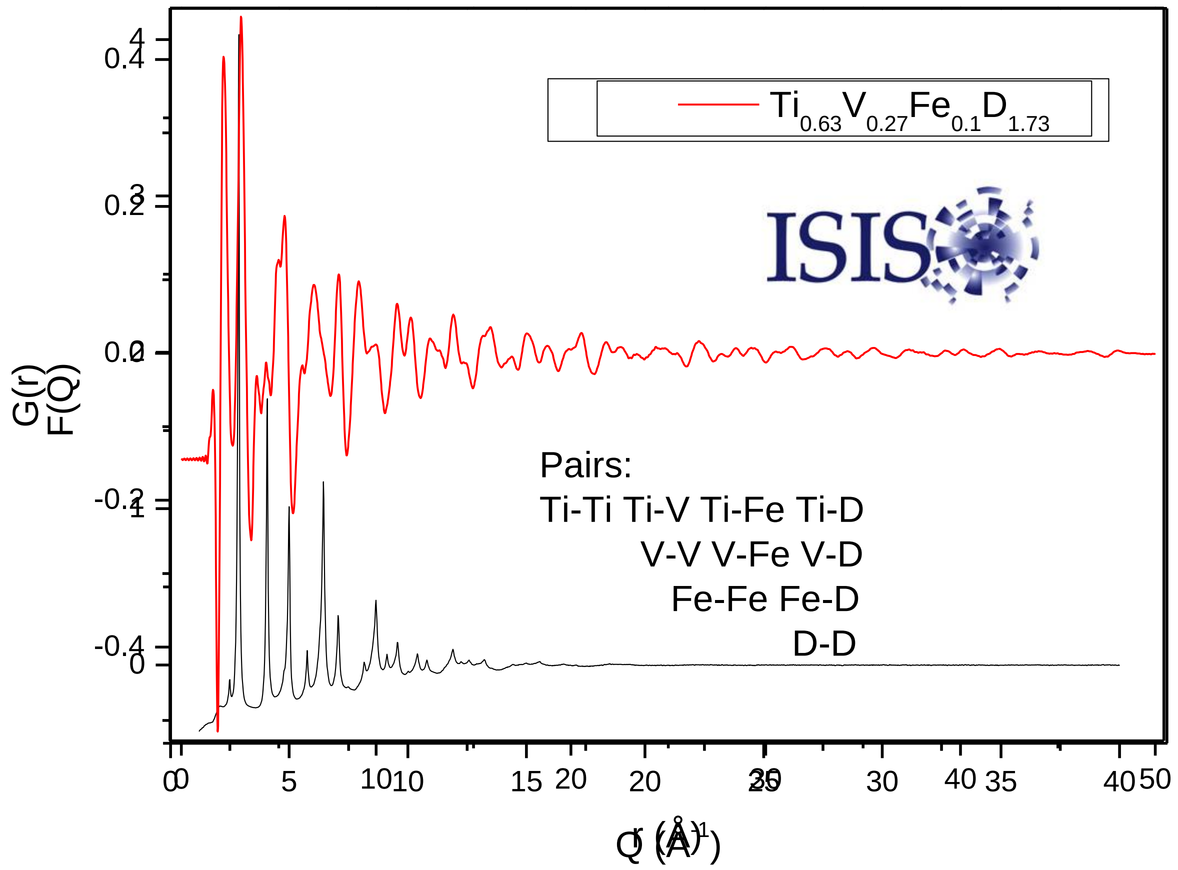

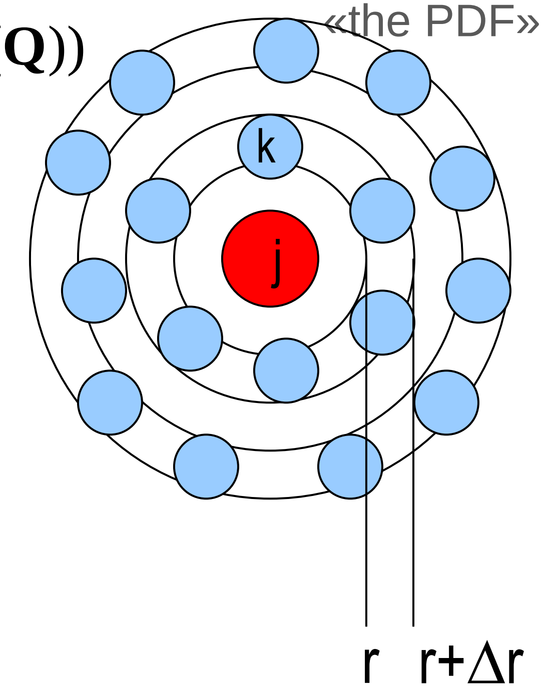

Partial PDF

$$g_{jk}(r) = \frac{\rho_k(r)}{\rho_k^{overall}}$$

Pair distribution function - PDF

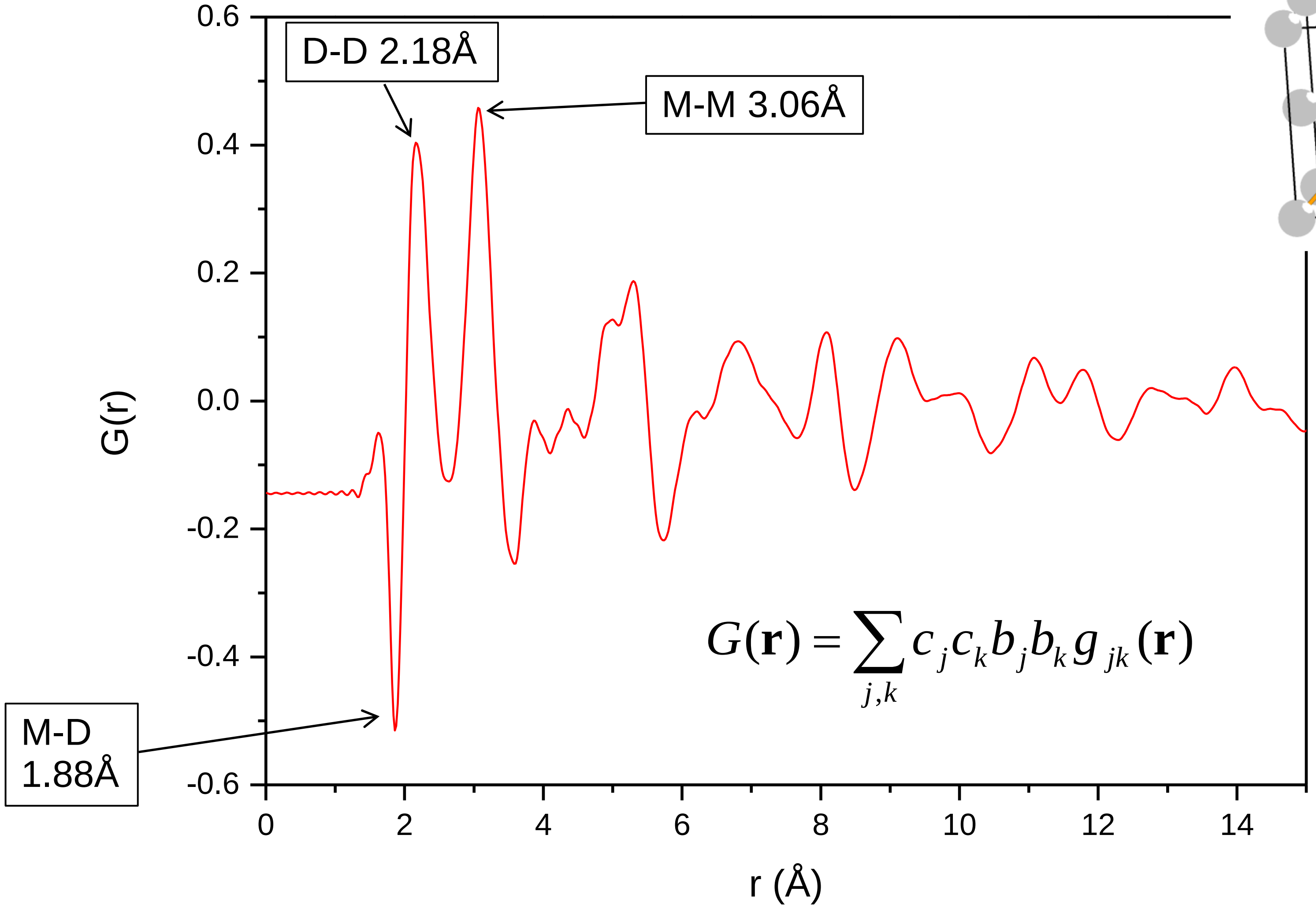

$$G(\mathbf{r}) = \sum_{j,k} c_j c_k b_j b_k g_{jk}(\mathbf{r})$$

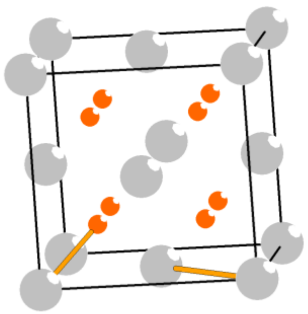

Scattering lenghts

b(Ti) = -3.4 fm
b(V) = -0.3 fm
b(Fe) = 9.5 fm
b(D) = 6.7 fm

RMCProfile modelling package (ISIS)

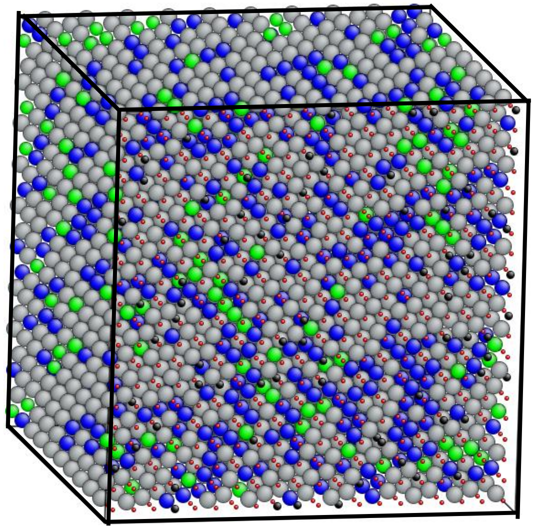

- 10x10x10 supercell
- 10800 atoms
- 1200 vacancies
- Swap M1-M2
- Swap D-Vac
- D-D and M-D cutoffs

http://www.rmcprofile.org/

RMCProfile Fit

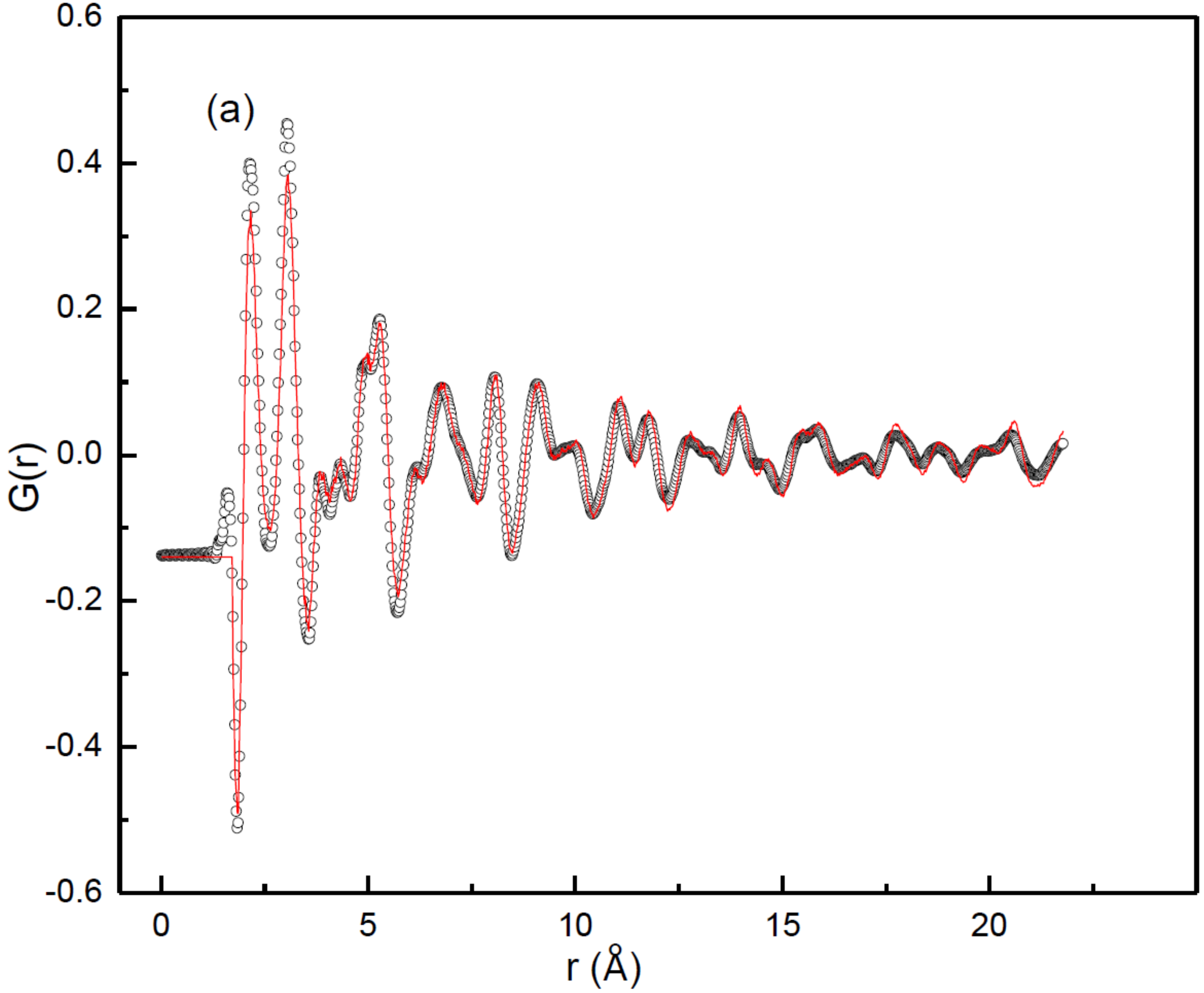

Partial PDFs

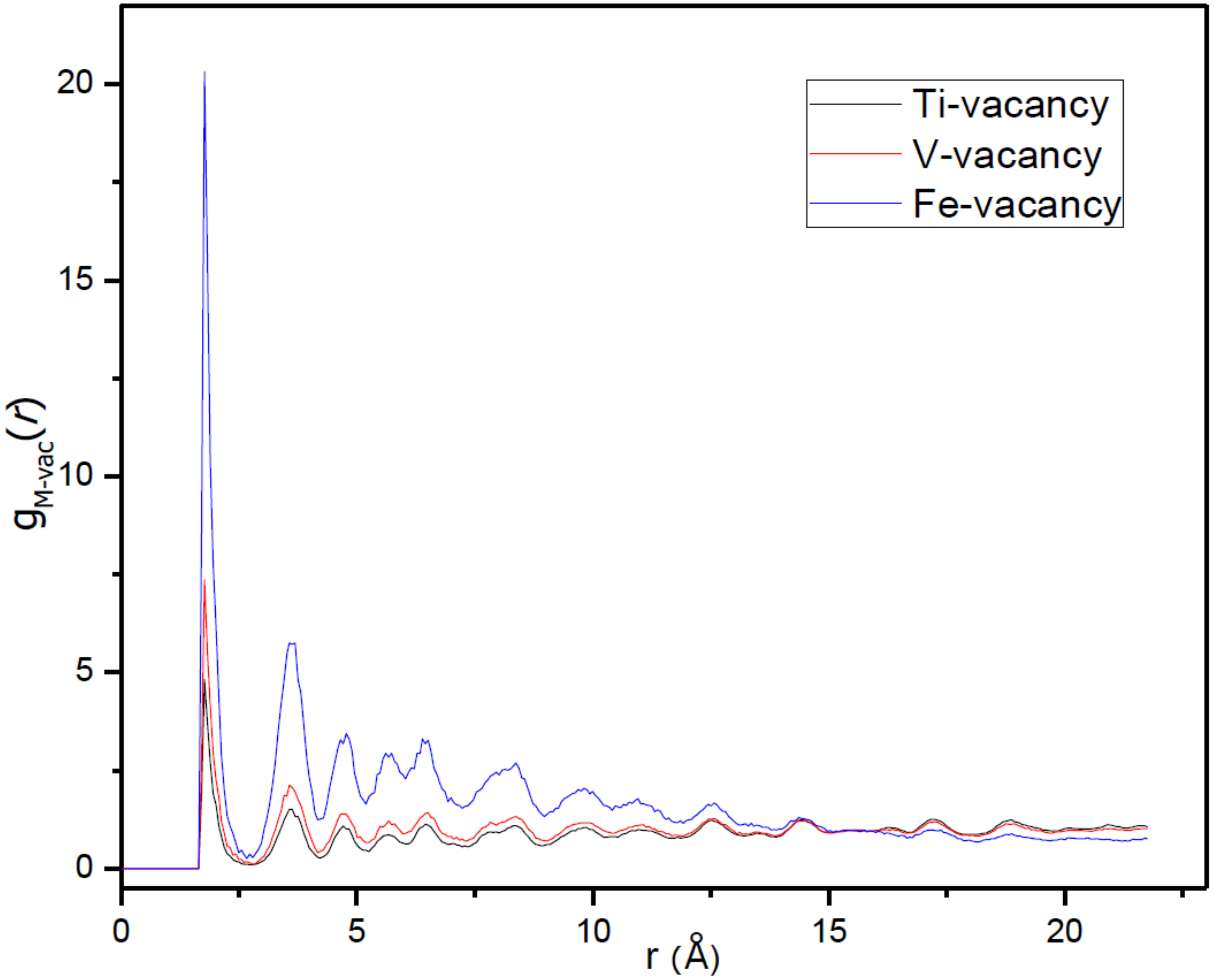

Partial PDFs

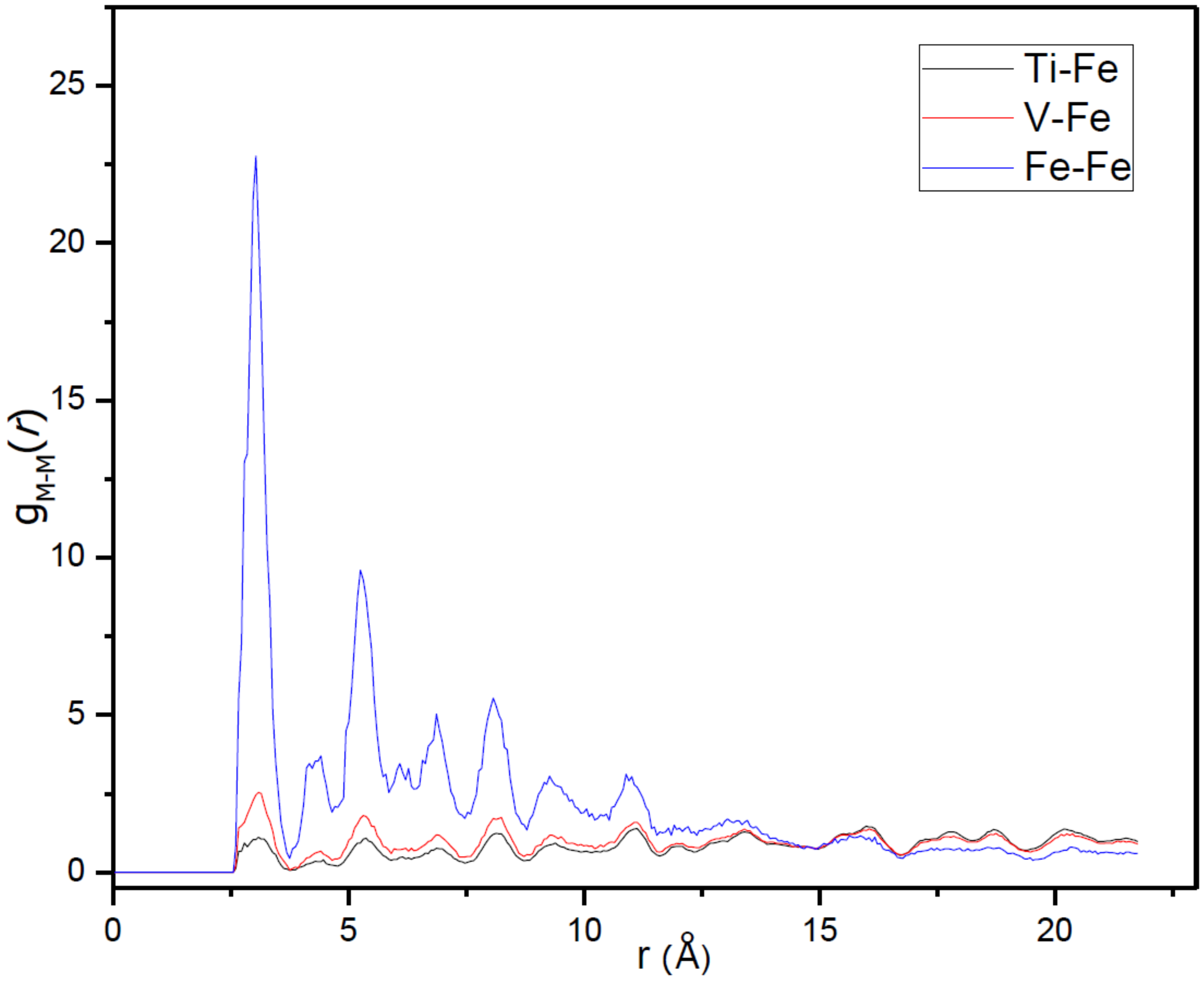

RMC models: Fe-vacancy

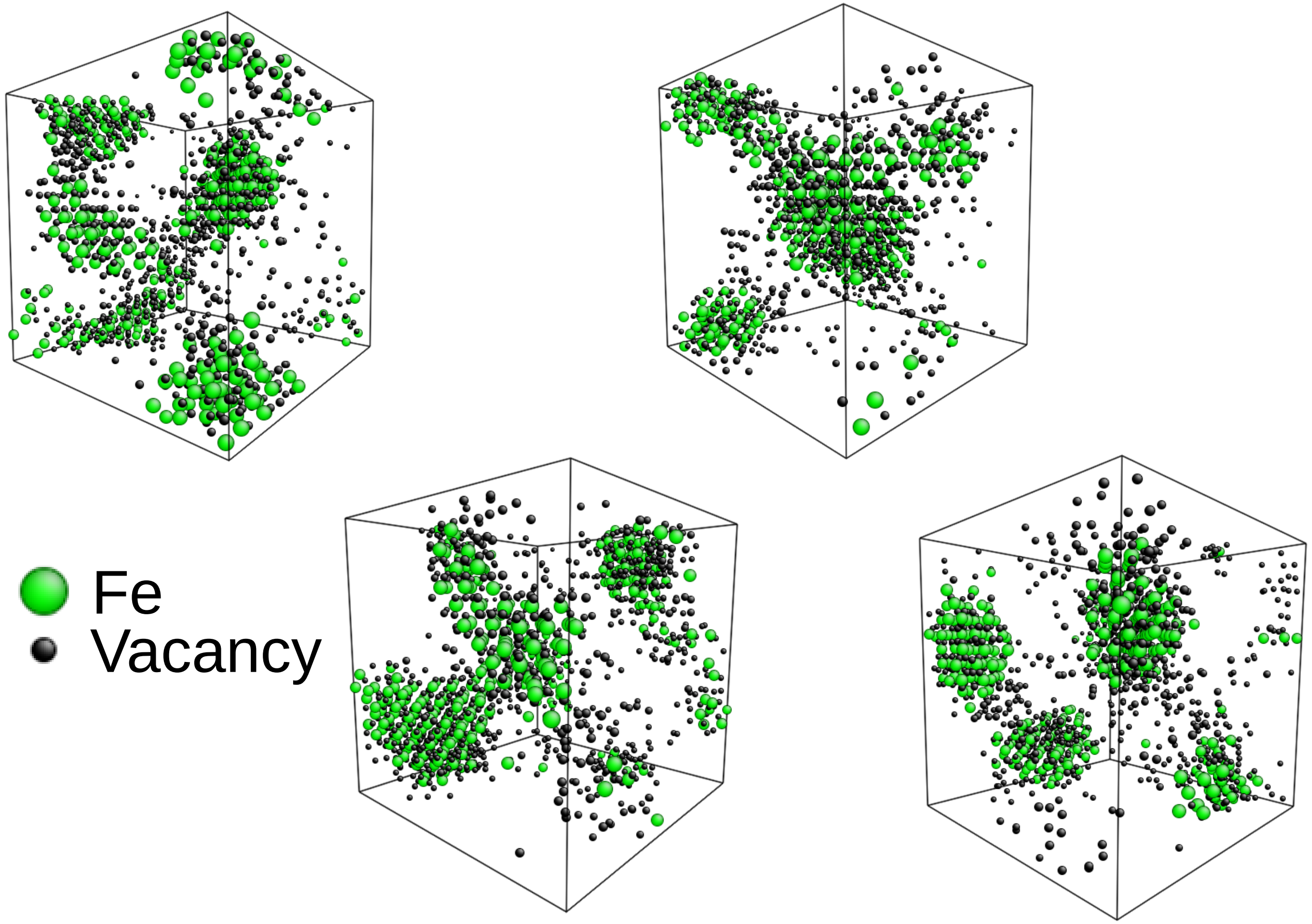

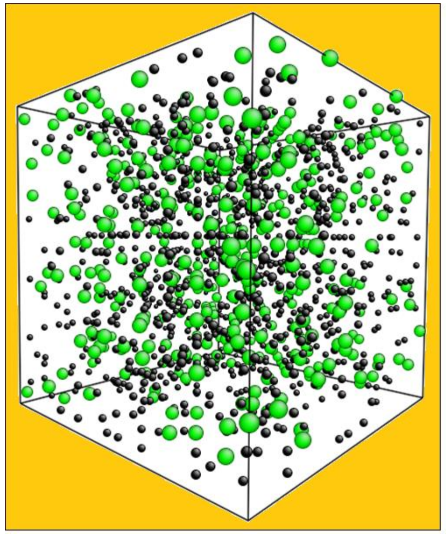

Initial model

Conclusion

- Ferrovanadium can greatly reduce the cost of V-based bcc alloys for hydrogen storage, allthough with the penelty of reduced capacity.

- Fe form clusters which are unfavorable for hydrogen in $(Ti_{0.7}V_{0.3})_{0.9}Fe_{0.1}D_{1.73}$.

Conclusion

- Total scattering can provide complementary information to Rietveld refinement.

- The local structures of the disordered deuterides resemble those of the ordered phases at length scales of a few Ångstrøm.